BNL-73104-2004-JA

JOURNAL OF GEOPHYSICAL RESEARCH, VOL. 109, D17306, doi:10.1029/2003JD004311, 2004

Origin and properties of plumes of high ozone observed during the Texas 2000 Air Quality Study (TexAQS 2000)

P. H. Daum,[1] L. I. Kleinman,[1] S. R. Springston,[1] L. J. Nunnermacker,[1] Y.-N. Lee,[1] J. Weinstein-Lloyd,[2] J. Zheng,[3] and C. M. Berkowitz[4]

Received 31 October 2003; revised 17 June 2004; accepted 28 June 2004; published 14 September 2004.

[1] The Department of Energy (DOE) G-1 research aircraft made flights on 13 days during the month long Texas 2000 Air Quality Study (TexAQS 2000) to understand the sources and formation mechanism of the very high concentration O_3 plumes that are frequently observed in the Houston metropolitan area during the late summer. On six of those days the aircraft sampled plumes exhibiting O_3 concentrations in excess of 150 ppbv at a number of different locations in and around the greater Houston area. The composition of these plumes differed significantly from those typically observed in other urban areas, exhibiting unusually high concentrations of hydrocarbon oxidation products such as HCHO and photochemical product species such as peroxides. Estimates of the integrated formation efficiency of O_3 with respect to NO_x, OPEx, indicate that O_3 had been formed in these high concentration plumes with efficiencies ranging between 6.4 and 11 ppbv O_3 per ppbv of NO_x consumed. Without exception, back trajectories from the locations where these high O_3 plumes were observed passed over, or in close proximity to, sources of NO_x and hydrocarbons surrounding the Houston Ship Channel. Calculations of instantaneous ozone formation rates and efficiencies using a box model constrained by measurements of stable species showed that ozone formation over and around the Houston Ship Channel could be very rapid (instantaneous rates up to 140 ppbv/h) and very efficient (OPEx up to 28) and, in some instances, limited by the availability of NO_x. High concentrations of reactive hydrocarbons and NO_x emitted by industries in this area appeared to be the cause of these high rates and efficiencies. Examination of the distribution of photochemical product distributions in the high O_3 plumes arising from Ship Channel emissions suggests that O_3 formation in these plumes was much more NO_x limited than in typical urban plumes at equivalent times in their evolution. However, chemical/transport model simulations with realistic emissions inventories are needed to resolve the question of whether a NO_x- or hydrocarbon-based control strategy would be most effective at controlling greater Houston O_3 concentrations. *INDEX TERMS:* 0345 Atmospheric Composition and Structure: Pollution—urban and regional (0305); 0368 Atmospheric Composition and Structure: Troposphere—constituent transport and chemistry; 0365 Atmospheric Composition and Structure: Troposphere—composition and chemistry; *KEYWORDS:* urban pollution, ozone formation, industrial hydrocarbons

Citation: Daum, P. H., L. I. Kleinman, S. R. Springston, L. J. Nunnermacker, Y.-N. Lee, J. Weinstein-Lloyd, J. Zheng, and C. M. Berkowitz (2004), Origin and properties of plumes of high ozone observed during the Texas 2000 Air Quality Study (TexAQS 2000), *J. Geophys. Res.*, *109*, D17306, doi:10.1029/2003JD004311.

1. Introduction

[2] The TexAQS 2000 air quality study was conducted during the late summer (15 August to 15 September 2000) to investigate the combined chemical conversion and meteorological transport processes that lead to the frequent occurrence of O_3 concentrations well in excess of the current National Ambient Air Quality (NAAQS) 120 ppbv 1 hour standard for O_3 in the city of Houston and the surrounding counties. The population of the greater Houston metropolitan area is over four million people and due to the absence of major public transportation facilities this results in large quantities of emissions from mobile sources. Houston, and the surrounding area, is also home to one of the largest concentrations of petrochemical industries in the U.S. Much of this industry is located in close proximity to the Houston Ship Channel, which runs from almost the center of Houston to Northern Galveston Bay, but the city

[1]Environmental Sciences Department, Atmospheric Sciences Division, Brookhaven National Laboratory, Upton, New York, USA.
[2]Chemistry and Physics Department, State University of New York at Old Westbury, Old Westbury, New York, USA.
[3]Institute for Terrestrial and Planetary Atmospheres, State University of New York at Stony Brook, Stony Brook, New York, USA.
[4]Atmospheric Sciences and Global Change Division, Pacific Northwest National Laboratory, Richland, Washington, USA.

Copyright 2004 by the American Geophysical Union.
0148-0227/04/2003JD004311$09.00

can also be affected by transport of emissions from the concentration of petrochemical industries in Texas City to the SSE of Houston and from the many isolated petrochemical facilities scattered about the area. Of interest to the present study is the concentration of industries producing low molecular weight alkenes, particularly ethene and propene. It is estimated that as much as 40% of the world's production capacity for these compounds is found in the Houston-Galveston-Brezoria area.

[3] A unique characteristic of the Houston O_3 problem is the observation of short duration (hours), spatially localized, high concentration O_3 events (>150 ppbv) that occur even when background O_3 concentrations are modest (30–50 ppbv). The observation of these high O_3 events is not restricted to the area about the intense source region surrounding the Houston Ship Channel or Texas City but have been found to occur at multiple locations in the metropolitan area. This differs from O_3 exceedances observed in other areas of the country which typically occur over entire metropolitan areas, persist for many hours if not days, and particularly on the U.S. East Coast, involve interurban if not regional transport of ozone and its precursors.

[4] Previous reports of findings from the TexAQS 2000 study have shown that petrochemical facilities emit large amounts of NO_x and hydrocarbons to the atmosphere and that these emissions consistently result in the rapid and efficient production of high concentrations of O_3 [*Kleinman et al.*, 2002a; *Ryerson et al.*, 2003; *Daum et al.*, 2003]. A major source of the hydrocarbon reactivity for formation of these high ozone concentrations was observed to be ethene and propene [*Kleinman et al.*, 2002a; *Ryerson et al.*, 2003; *Wert et al.*, 2003; *Daum et al.*, 2003] the emissions of which have been estimated to be as much as a factor of 10 or more larger than those reported in current emissions inventories [*Ryerson et al.*, 2003]. In a modeling study of the composite Houston urban and Ship Channel plumes sampled on 1 September 2000, *Wert et al.* [2003] estimate that ethene and propene emissions alone could account for the high concentrations of O_3 (200 ppbv) and HCHO (30 ppbv) observed in this plume some four hours downwind of the source region.

[5] In an earlier study [*Daum et al.*, 2003] we examined O_3 formation on a day (29 August 2000) when stagnation allowed the accumulation of O_3 and O_3 precursors over and around the industrialized Ship Channel source region. Here we examine O_3 formation on all of the G-1 flight days during which an O_3 plume in excess of 150 ppbv was encountered by the aircraft. This included six of the thirteen G-1 flight days. These high O_3 plumes were found at a number of different locations in the Houston metropolitan area and the question arises as to whether they were also associated with emissions emanating from the Ship Channel industries and whether the properties of these plumes were similar to those found in the 29 August 00 case study. To address these questions, we first show the geographical location of these plumes and conduct a back trajectory analysis that shows that all traveled over the source region surrounding the Houston Channel at some point in their immediate past history. We next examine the geographical distribution of hydrocarbon reactivity and ozone formation rates on several of the days, and link regions of high hydrocarbon reactivities and formation rates to regions where high O_3 concentrations were observed. We conclude, similar to the 29 August 2000 case study, that emissions from one or more of the many industrial complexes in the Ship Channel were associated with the occurrence of all of these plumes of high O_3. Photochemical product distributions are examined to give insight as to whether the observed peak O_3 concentrations were limited by the availability of NO_x or hydrocarbons.

2. Experiment

[6] Measurements presented here were conducted with the DOE Gulfstream G-1 aircraft, an intermediate-sized, twin turboprop aircraft equipped with a variety of instrumentation for the measurement of ozone, aerosols, ozone/aerosol precursors, and a variety of photochemical product species. The flight strategy was dictated by the need to avoid the crowded airspace around the two major airports serving Houston one of which (Hobby Airport) is just to the south of the center of Houston's urban area and one (Bush International) to the north, and the need to sample plumes from the Houston urban area and from the industrialized region around the Houston Ship Channel at various stages in their development. The standard program flight track consisted of a figure eight pattern with the two airports respectively at the centers of the two lobes of the eight. The track took the aircraft right over the center of Houston and over the industrialized Ship Channel to the east of Houston; the lobes were expanded as dictated by conditions. A limited amount of data (O_3 and hydrocarbons) from the Baylor Twin Otter is also used in this analysis. The flight strategy of the Twin Otter was focused on source regions around the Ship Channel, Texas City and isolated facilities to the south of Houston, and on the overnight accumulation of O_3 and O_3 precursors over Galveston Bay. A description of the measurements relevant to the data discussed here are given below.

2.1. Aircraft Measurements

[7] Measurements made on the G-1 during the TexAQS 2000 Study are discussed in some detail elsewhere [*Daum et al.*, 2003]. Briefly, oxides of nitrogen were measured using a three channel NO/O_3 chemiluminescence instrument measuring NO, NO_2 and NO_y as described by *Nunnermacker et al.* [1998] except for the placement of the molybdenum NO_y converter external to the aircraft to minimize losses of HNO_3. The efficiencies of the photolytic NO_2 converter and the molybdenum NO_y converter averaged 34.6% σ = 0.9%, and 99.6% σ = 0.3%, respectively. The uncertainty in the measured concentrations for 10 s averaged data is estimated to be 20 ppt ± 10% of the NO concentration, 100 ppt ± 15% of the NO_2 concentration, and 250 ppt ± 10% of the NO_y concentration. CO measurements were made with a modified nondispersive infrared detector (Thermo Environmental Instruments, Model 48). Estimated uncertainty in the CO concentrations is 50 ppbv ± 15% of the measured concentration. Although highly uncertain, CO measurements are used here only in the calculation of hydrocarbon reactivity, and because CO is such a small fraction of that reactivity, the high degree of uncertainty is not significant for the analysis reported here. O_3 was

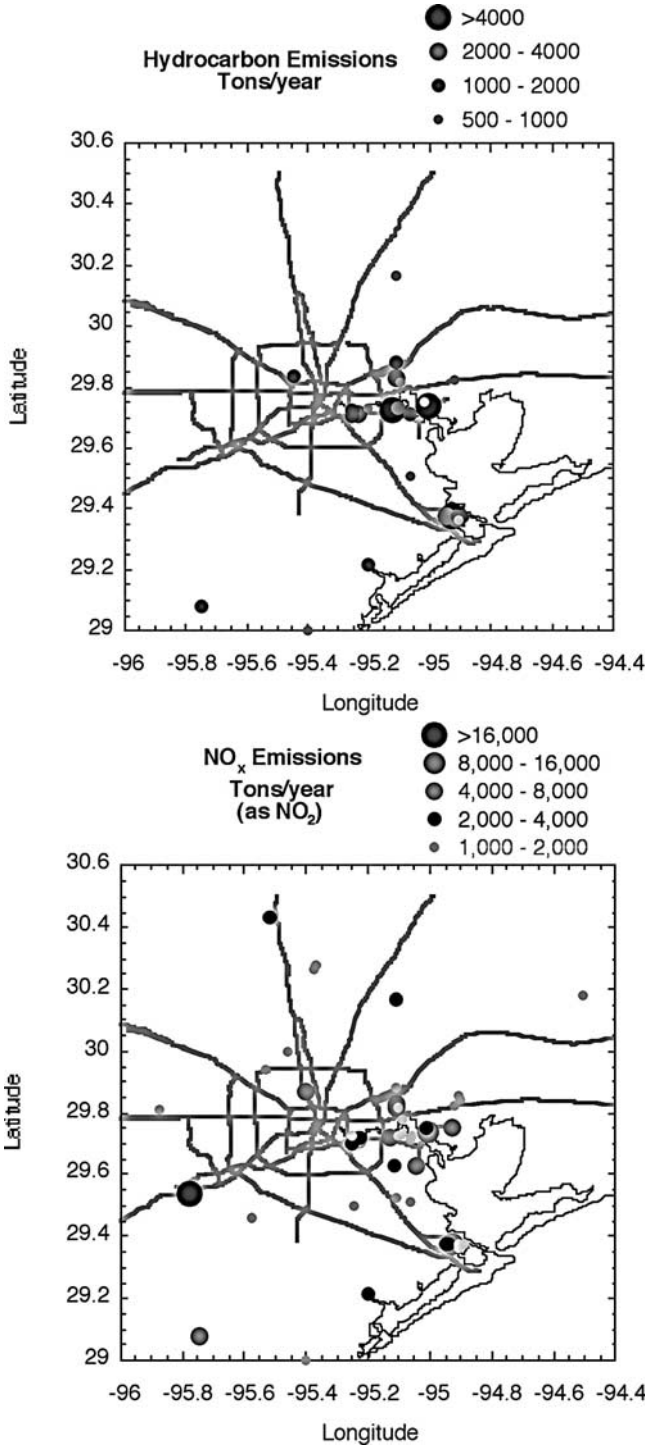

Figure 1. Geographic distribution of hydrocarbon and NO_x point sources in the Houston/Galveston area. Sources of hydrocarbons below 500 tons per year and NO_x below 1000 tons per year are not shown. See color version of this figure at back of this issue.

measured using a UV absorption detector (Thermo Environmental Instruments, Model 49-100). The estimated uncertainty in the measured O_3 concentration is 5 ppbv ± 5% of the measured concentration for 10 s averaged data. Peroxides were measured by scrubbing followed by derivitization and fluorescent detection [*Weinstein-Lloyd et al.*, 1998]. Uncertainty for total peroxides is estimated to be ±15%. Formaldehyde was measured by aqueous scrubbing, and chemical derivitization followed by HPLC separation and UV-Vis detection. Measurement uncertainty was estimated to be ±12% [*Lee et al.*, 1998] on the basis of calibrations using aqueous phase standards; inlet losses, if any, are unknown. Results of the single intercomparison flight of the G-1 and the NOAA/NCAR Electra aircraft measurements of O_3, NO, NO_2, SO_2, and CO conducted during the program are discussed by *Sueper et al.* [2002]. Hydrocarbons were measured by canister collection followed by GC/FID separation and detection [*Rudolph and Khedim*, 1985; *Rudolph*, 1999].

[8] O_3 measurements from the Twin Otter reported here were made using a UV absorption detector (Thermal Environmental Instruments, Model 49-100), estimated uncertainty 5%. Nitrogen dioxide measurements used in the calculation of Ox (defined as O_3 + NO_2) were highly uncertain, perhaps by as much as 50%; hydrocarbons were measured by canister collection followed by GC/FID separation and detection [*Harley et al.*, 2001].

2.2. Emissions Maps

[9] The geographic distribution of point sources emitting hydrocarbons, and NO_x for the region surrounding Houston are shown in Figure 1 (see U.S. Environmental Protection Agency, AIR Data database, available at http://www.epa.gov/air/data). The densest region of hydrocarbon sources is clustered about the Houston Ship Channel just to the east of downtown Houston. These emissions are associated with the many chemical processing plants that manufacture a vast array of products for use by industry, but also use the Ship Channel as a conduit for both raw materials and finished products. A much smaller cluster of emissions is found to the south of Houston around the Texas City industrial complex. The remainder of the emissions come principally from isolated petrochemical facilities to the southeast of Houston near the Gulf Coast. The geographic distribution of NO_x emissions is similar to the one for hydrocarbon emissions with clusters of high emissions around the Ship Channel and Texas City and a scattering of smaller sources elsewhere. The NO_x emissions from these industrial facilities originate principally from the combustion of fossil fuels for process heat generation, electric power production, and flaring of excess hydrocarbons. The Parrish Power Plant just to the SW of Houston is the largest single point source of NO_x in the area but emits little if any hydrocarbons. It is thought that the NO_x emissions from these point sources are reasonably well represented in current emissions inventories, but that hydrocarbon emissions are not [*Ryerson et al.*, 2003; *Wert et al.*, 2003; *Karl et al.*, 2003].

2.3. Model Calculations

[10] Interpretation of the G-1 data presented here relies heavily on calculations conducted using a constrained steady state (CSS) box model that determines the concentrations of NO_2 and free radicals that are in steady state with the observed mixture of trace gases. Observations used in the model include the concentrations of O_3, H_2O, NO, CO, speciated hydrocarbons, HCHO, SO_2, H_2O_2 and organic peroxides; pressure and temperature; and, actinic flux de-

rived from Eppley radiometer measurements as described by *Kleinman et al.* [2002a, 2002b]. The gas phase photochemical mechanism is based upon the regional acid deposition model RADM II [*Stockwell et al.*, 1990] for the oxidation of anthropogenic hydrocarbons and upon the condensed mechanism of *Paulson and Seinfeld* [1992] for the oxidation of isoprene. The model computes quantities such as the instantaneous rate ($P(O_3)$) and efficiency (OPEx) of ozone formation, and the formation rates for nitrates (L_N) and peroxides (L_R). Details of the model and its application to the analysis of O_3 formation in other studies can be found elsewhere [e.g., *Kleinman et al.*, 1997, 2000, 2001, 2002b; *Daum et al.*, 2000a, 2000b, 2003]. Calculations correspond to times when hydrocarbon canister samples were collected and for this reason are restricted in number.

[11] Model output is interpreted using approximate equations that have been developed previously [*Sillman et al.*, 1990; *Kleinman et al.*, 1997; *Daum et al.*, 2000a, 2000b; *Kleinman et al.*, 2000, 2001]. Much of the interpretation of O_3 formation rates is done here in the context of the quantity L_N/Q which represents the fraction of radicals removed by radical-NO_x reactions such as $OH + NO_2 \rightarrow HNO_3$ (where Q is the primary radical production rate). L_N/Q is an indicator variable for NO_x or hydrocarbon sensitive O_3 formation. When L_N/Q is near zero, O_3 formation is NO_x sensitive and the principal chain termination reaction is formation of peroxides. When L_N/Q is near 1, O_3 formation is hydrocarbon sensitive, and the principal chain termination reaction is formation of HNO_3. The transition between hydrocarbon and NO_x sensitive O_3 formation occurs when $L_N/Q = 0.5$. The variables controlling L_N/Q are discussed by *Kleinman et al.* [2001].

3. Results and Discussion

3.1. Spatial Distribution of Ozone Concentrations

[12] Spatial distributions of oxidant concentrations, Ox concentrations on the days when O_3 concentrations in excess of 150 ppbv were measured by the G-1 aircraft are shown in Figure 2. As indicated in Figure 2, peaks of high Ox concentration observed by the G-1 tended to be very localized, and for the most part to be superimposed upon regional ozone concentrations that were modest though variable. On most of these days, regional Ox concentrations were below 80 ppbv, and in some cases as low as 30–40 ppbv. The one exception is 31 August when background Ox concentrations were between 80 and 100 ppbv. In almost all cases plume concentrations exceeded regional levels by more than 100 ppbv (19, 21, and 26 August), and in some cases 150 ppbv (29 August). This extreme difference between plume and regional concentrations and the localized geographic distribution of these plumes indicates that they probably originate from a localized region of high emissions of ozone precursors. This contrasts to the situation in the eastern U.S. where high background concentrations have an important role in determining whether NAAQS O_3 levels are exceeded and where high ozone concentrations during an episode tend to be widely distributed affecting multiple metropolitan areas nearly simultaneously [e.g., *Ryan et al.*, 1998; *Zhang et al.*, 1998].

[13] As indicated by Figure 2, these plumes of high Ox concentration appeared at various locations in and around Houston. On 19 August and 26 August, plumes were observed 30–60 km NE of Houston; on 21 August, they were observed over downtown Houston and to the west; on 29 August, they were to the east of Houston and over northern Galveston Bay; on 31 August, they were over the city and east to Galveston Bay, and on 6 September, they were to the southwest of Houston. The appearance of these plumes at these various locations suggests that sources of O_3 precursors responsible for these high Ox concentrations were not necessarily associated with the location where these plumes were observed. Surface observations were generally consistent with the aircraft observations. However because of the relative sparseness of the surface sites and the clustering of their location around the Houston urban center, there were a number of days when the surface network missed plumes of high O_3 that were observed by the aircraft.

3.2. Back Trajectory Analysis

[14] In this section we examine back trajectories for all of the high O_3 plumes during the six G-1 flights when concentrations were in excess of 150 ppbv. Trajectories were calculated using meteorological fields derived from the wind profiler network that was set up as part of the experiment [*Daum et al.*, 2003]. Particles were advected at 15 minute time steps using wind fields interpolated between the hourly observations. The starting point for the back trajectories was the location of the center of the plume(s) in which O_3 concentrations exceeded 150 ppbv. Starting times for the back trajectories were rounded off to the nearest hour.

[15] Back trajectories for all of the high ozone plumes sampled by the G-1 during the study are superimposed on the flight track/Ox distribution maps shown in Figures 2a–2f. Symbols on the plots represent time intervals of one hour. Examination of the back trajectories indicates that without exception, air masses in which high O_3 concentrations were observed passed over, or in close proximity to point sources of emissions around the Houston Ship Channel and Galveston Bay (Figure 1). The Ox distribution and back trajectories for the afternoon flight of 19 August shown in Figure 2a serves as a good example. A localized region of high ozone concentrations were observed northeast of downtown Houston during the midafternoon. Back trajectories from different portions of this pool of high ozone concentration all cross the Houston Ship Channel where the major sources are located but at different times and locations, implying that emissions from different sources processed for varying lengths of time contribute to this region of high ozone. For example, the high ozone plume sampled north of the Ship Channel on 19 August actually consists of two plumes, one of which is about 8 hrs downwind of the source region and the other about 4 hours downwind; NO_x concentrations in the former are <2 ppbv and in the latter are 15 ppbv consistent with the transit times from source regions that may be inferred from the back trajectories.

[16] Another feature of the back trajectories that has bearing both on sources of ozone precursors and on plume Ox concentrations is well illustrated by the back trajectories

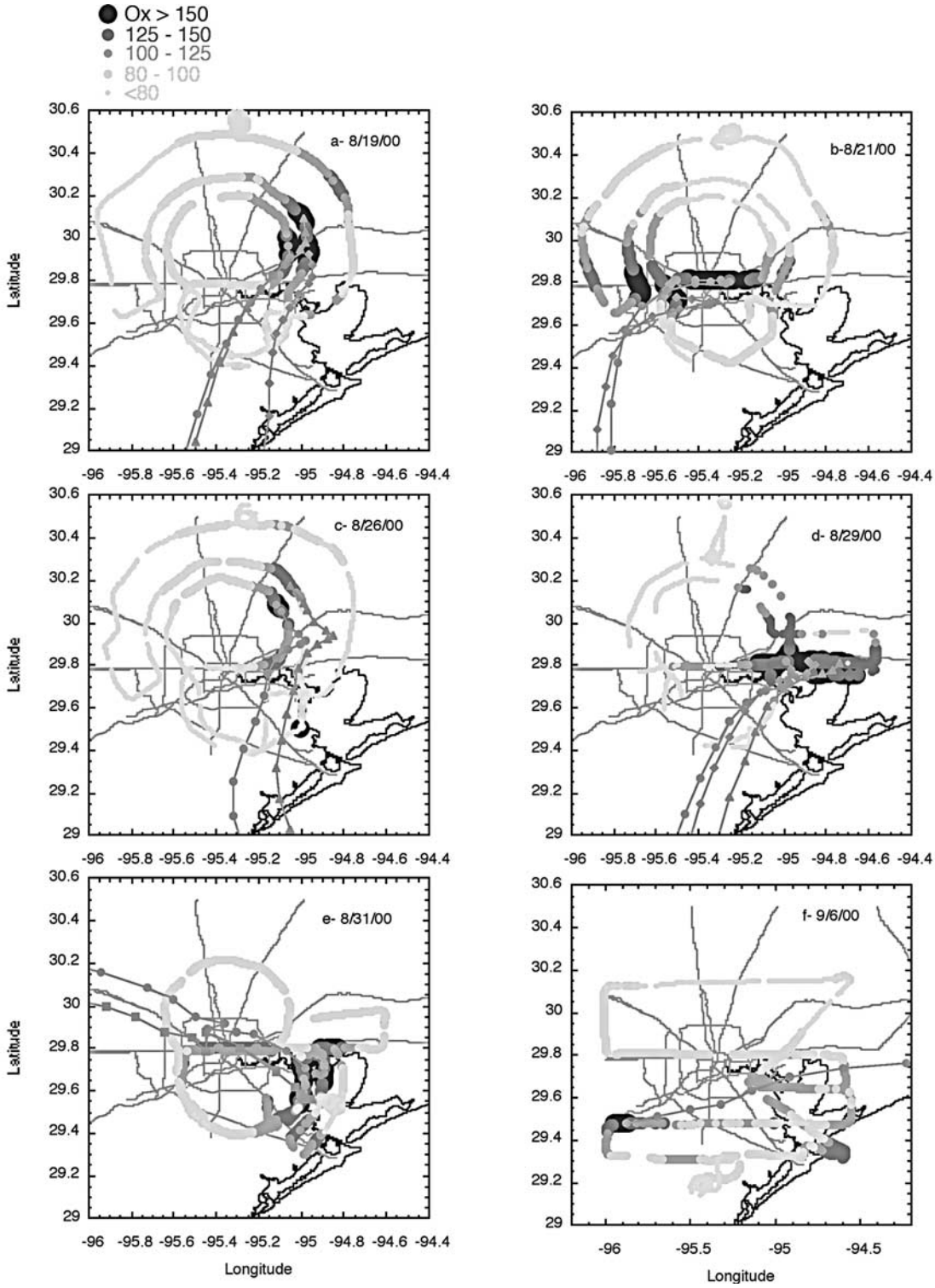

Figure 2. Geographic distribution of Ox for G-1 flights during which O_3 concentrations were >150 ppbv. Blue lines are back trajectories from the indicated locations of high Ox. Symbols on the trajectories are spaced at 1-h intervals. Read 8/19/00 as 19 August 2000. See color version of this figure at back of this issue.

observed on 21, 26, 29, and 31 August. Using the back trajectories from 21 August as an example, we see that the air mass in which the high ozone was observed, was in the vicinity of the region of sources surrounding the Ship Channel some 2–5 hours prior. Note also that the air mass underwent a period of very slow motion (essentially stagnation) in the source region for a period of 3–4 hours. This allowed the accumulation of emissions from sources in this

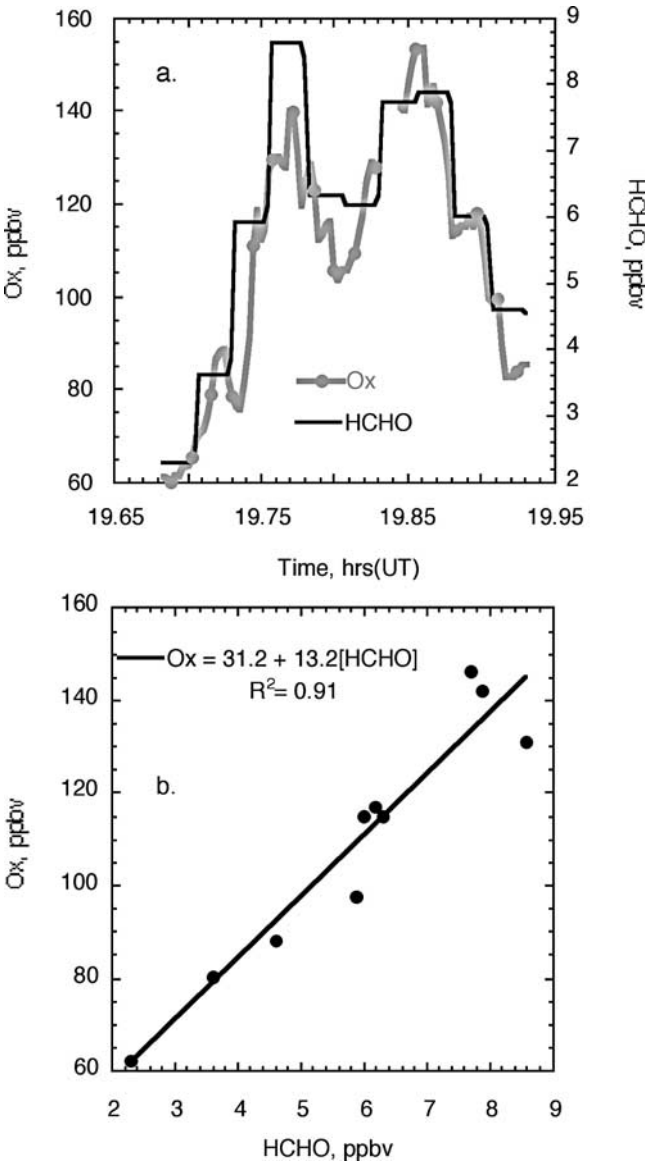

Figure 3. Ox and HCHO concentrations observed in the high O_3 plume on the afternoon flight of the G-1 on 26 August 2000. (a) Time variation of HCHO and Ox. (b) Correlation of HCHO and Ox; for purposes of this plot, Ox concentrations have been averaged over the sampling interval of the HCHO instrument.

area which were subsequently processed to generate the O_3 that was observed. Prior to the period of stagnation, trajectories were from the southwest. A similar period of stagnation pertained for O_3 plumes observed on other days when high O_3 concentrations were observed, e.g., 19, 26, 29, and 31 August. On 29 August, plumes were observed just north of the Ship Channel. Back trajectories for 29 August (Figure 2d) indicate that this was a consequence of an extended period of stagnation that allowed accumulation and reaction of precursors to form locally in the source region. The 29 August data are examined in detail elsewhere [*Daum et al.*, 2003]. On 6 September no period of stagnation was observed, but back trajectories went over the source region, and apparently winds speeds were sufficiently low that high O_3 concentrations formed.

[17] A conceptual model of the meteorological conditions associated with the observation of high O_3 in Houston, consistent with our observations, has been developed [*Nielson-Gammon*, 2002]. Briefly, weak synoptic winds from any direction from the N to the SW carry emissions from the source region offshore out over Galveston Bay. If the synoptic flows are weak, a period of stagnation occurs as differential land/water solar heating causes the development of a driver that opposes the offshore flow. As the land/water temperature differential increases, a sea breeze develops that carries the air mass back over land. The exact path that the air mass takes is determined by the interaction of the forces driving the synoptic flow and those driving the land/sea breeze circulation.

3.3. Plume Characteristics

[18] The high concentration O_3 plumes observed during the TexAQS 2000 Study exhibited a number of characteristics that distinguish them from O_3 plumes found downwind of other point sources and other urban areas.

3.3.1. Composition

[19] From the perspective of composition these plumes were distinguished by very high, but variable concentrations of formaldehyde and by high concentrations of peroxides. An example of plume HCHO concentrations is shown for a high ozone plume observed on 26 August northeast of Houston (Figure 2c). Peak oxidant concentration in this photochemically mature plume (NO_x/NO_y ratio <0.2) is nearly 160 ppbv (Figure 3a). The formaldehyde concentration closely follows the oxidant concentration, and peaks at nearly 9 ppbv. The high degree of correlation between HCHO and the oxidant concentrations for the 26 August O_3 plume is explicitly shown in Figure 3b. Correlations observed in several of the other high O_3 plumes are shown Figure 4. Similar correlations with ozone concentrations were observed by *Wert et al.* [2003] in analysis of aircraft data collected by the NOAA/NCAR aircraft during the TexAQS 2000 program. The highest formaldehyde concentration, measured in the O_3 plume sampled on 29 August just north of the Ship Channel, was circa 30 ppbv [*Daum et al.*, 2003].

[20] That HCHO concentrations are so high in these plumes is significant as HCHO can serve both as a fuel for the formation of ozone and as a significant source of primary radicals through photolysis and subsequent formation of peroxy radicals for the initiation of the ozone formation process. In an analysis of the data collected on 29 August [*Daum et al.*, 2003], it was shown that HCHO photolysis can rival O_3 photolysis as a source of primary radicals in high ozone plumes sampled during TexAQS 2000. Although formaldehyde is emitted directly into the atmosphere by both natural and anthropogenic sources, such emissions are not thought to be nearly as significant as the HCHO that comes from the photodegradation of hydrocarbons in the atmosphere [*Wert et al.*, 2003, and references therein]. Important hydrocarbons from the perspective of HCHO formation are low molecular weight alkenes (ethene, propene and butenes) which are emitted from automobiles and industrial processes and isoprene which comes principally from biogenic sources.

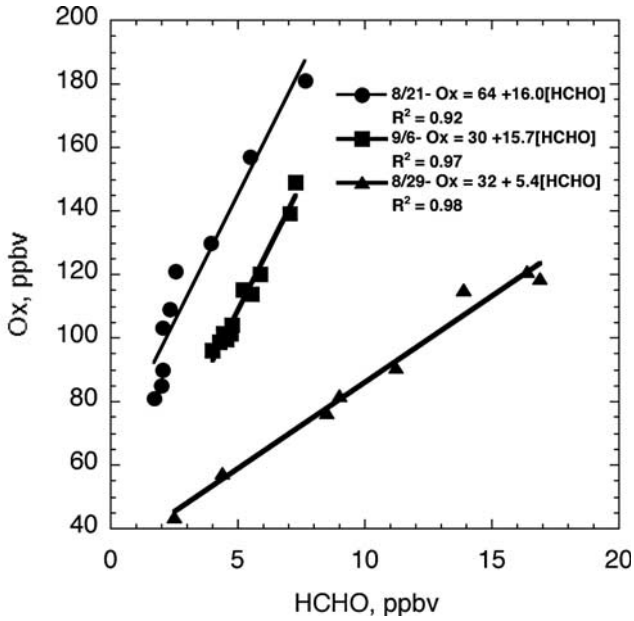

Figure 4. Ox/HCHO correlations observed in several of the high ozone plumes sampled by the G-1 during the TexAQS 2000 study.

[21] Ozone plumes sampled during TexAQS 2000 were also distinguished by their generally high peroxide concentrations. Examples of peroxide and the corresponding oxidant concentrations are shown in Figures 5 and 6 for plumes sampled on the afternoons of 19 and 26 August. For most urban plumes, sampled at equivalent times in their development [*Nunnermacker et al.*, 1998; *Weinstein-Lloyd et al.*, 1998], peroxide concentrations are anticorrelated with oxidant concentrations. This is also true for fossil-fueled power plant plumes [*Jobson et al.*, 1998]. However,, in the two examples shown, which are representative of the behavior that was observed in nearly all of the high ozone plumes sampled during the program, peroxide concentrations increase with increasing oxidant concentrations, occasionally reaching very high values (11–13 ppbv on 19, 21, and 29 August; 16 ppbv on 31 August).

[22] Peroxides are produced in the atmosphere by the combination of peroxy radicals, and destroyed in clear air by photolysis and reaction with OH. When NO_2 concentrations are high and the ratio of reactivities of the hydrocarbon and NO_2 reactions with OH is low, peroxy radical concentrations are kept low by loss of radicals through reaction of OH with NO_2 to form HNO_3, and peroxide is destroyed more rapidly than it can be formed. This leads to a peroxide deficit in urban plumes until most of the NO_x in the plume has been consumed [*Weinstein-Lloyd et al.*, 1998]. The observation of excess peroxide in the Houston high O_3 plumes so early in their lifetime suggests that the hydrocarbon to NO_x reactivity ratio is much higher than it is in a typical urban area, in turn suggesting that O_3 formation is much less hydrocarbon limited than is typical of an urban area. Indeed, detailed analysis of the data from 29 August [*Daum et al.*, 2003] showed that O_3 formation in the Houston urban plume was much more hydrocarbon limited than in the Ship Channel plumes. A further analysis of peroxide data relative to NO_x or hydrocarbon limitations to O_3 formation in Houston will be given below.

3.3.2. Ozone Formation Efficiency

[23] The efficiency of ozone formation with respect to NO_x, is an important metric for understanding ozone formation and developing effective control strategies. Under most urban plume conditions, the instantaneous efficiency of ozone formation, OPEx, is proportional to the ratio of the hydrocarbon to NO_2, OH reactivity [*Kleinman et al.*, 2002b; *Daum et al.*, 2000b]. As an urban plume matures, generating O_3 and consuming NO_x, the efficiency will rise because NO_x is consumed more rapidly than are hydrocarbons in the O_3 formation process. In previous studies of a number of urban areas, the integrated ozone production efficiency (not to be confused with OPEx which is an instantaneous quantity) derived from analysis of Ox/NO_z data (NO_z is

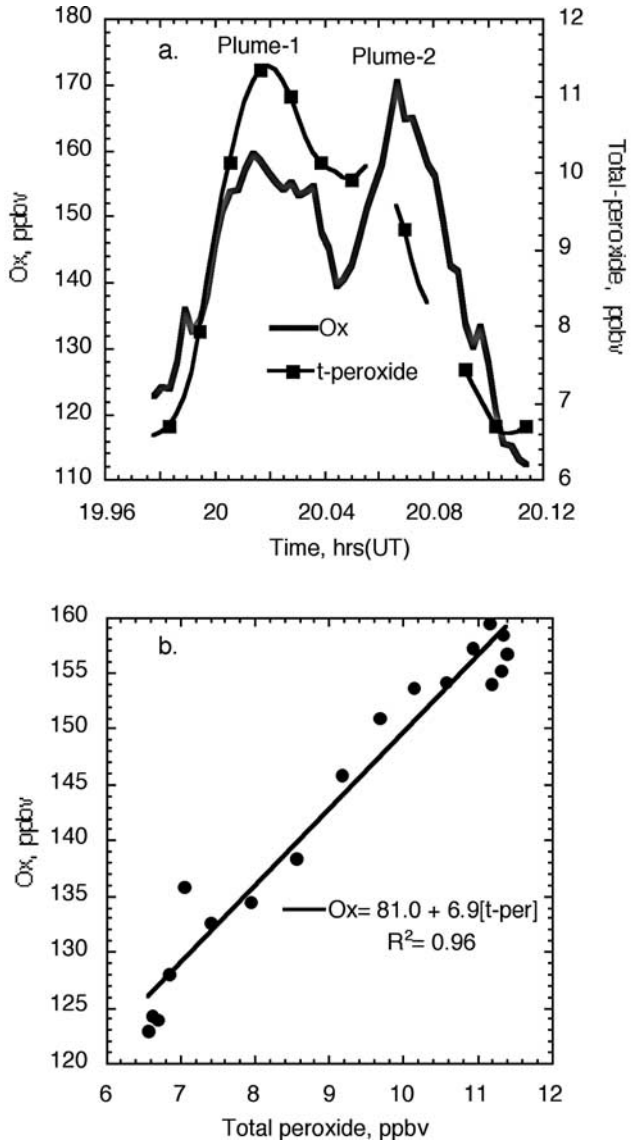

Figure 5. Peroxide and oxidant concentrations measured in the high O_3 plume sampled by the G-1 aircraft on 19 August 2000. (a) Time variation of Ox and peroxide. (b) Correlation of Ox and peroxide. Gaps in the peroxide record are due to instrument zeroes.

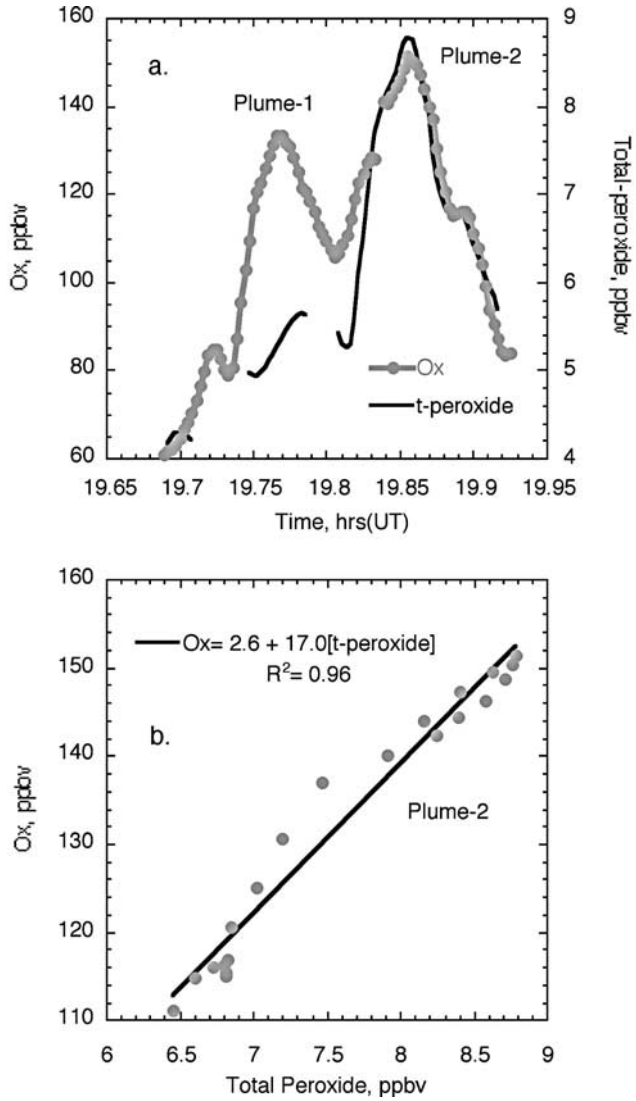

Figure 6. (a) Time plots of t-peroxide and oxidant concentrations in the high O_3 plume sampled by the G-1 on the afternoon of 26 August 2000. (b) Correlation plot of t-peroxide and oxidant for Plume-2 shown in Figure 6a. Gaps in the peroxide and Ox time records in are due to instrument zeroes.

defined as NO_x oxidation products including HNO_3, and organic nitrates such as peroxyacetylnitrate) range from 1 to 4 [*Nunnermacker et al.*, 1998; *Daum et al.*, 2000a, 2000b; *Kleinman et al.*, 2000] depending on the age of the plume when the efficiency was estimated. The higher values are associated with urban plumes that are photochemically mature exhibiting near maximum ozone concentrations, and the lower values associated with fresher plumes.

[24] Oxidant/NO_z relations for several of the high ozone plumes observed on different days during the Texas study are shown in Figure 7. The efficiencies shown in Figure 7 range from 6.5 to 9.5; on other high O_3 days, efficiencies as high as 11 were derived. On some days where multiple plumes of high ozone were observed efficiencies differed somewhat in the various plumes reflecting mostly differences in photochemical age with more aged plumes (lower NO_x/NO_y ratios) exhibiting higher efficiencies. On other days the plumes are apparently composed of air masses with somewhat different histories with regard to processing times and emissions sources, and exhibited regions with different efficiencies, but in all cases the efficiencies are considerably higher than have been observed in other urban areas and in plumes from other point sources such as power plant plumes. Since efficiencies for hydrocarbon limited ozone formation are proportional to the ratio of HC to NO_2 OH reactivity, the data presented above suggest that the ozone present in these plumes was formed under conditions where this ratio was considerably higher than in a typical urban plume. We will explore sources of this enhanced hydrocarbon reactivity in the next section.

3.4. Connecting Regions of High Ozone Concentrations to Ozone Formation Processes Occurring in the Precursor Source Regions

[25] In section 3.2 we showed that back trajectories from all of the high O_3 plumes sampled by the G-1 during the program went over, or in close proximity to the sources surrounding the Houston Ship Channel. In this section we will connect the properties of these O_3 plumes to O_3 formation processes that occur in the Ship Channel area where most of the precursors are added to the system, and where much of the O_3 formation may actually occur. There are examples from two days in this section: 26 August 2000, when emissions accumulated in the region of the Ship Channel in the morning and were then transported NE of Houston in the afternoon, and 21 August, when the accumulated emissions were transported over downtown Houston.

3.4.1. 26 August: A Ship Channel Plume

[26] Here data collected on 26 August 2000 will be examined focusing on the aircraft data collected on the morning and afternoon flights of the G-1. Back trajectories

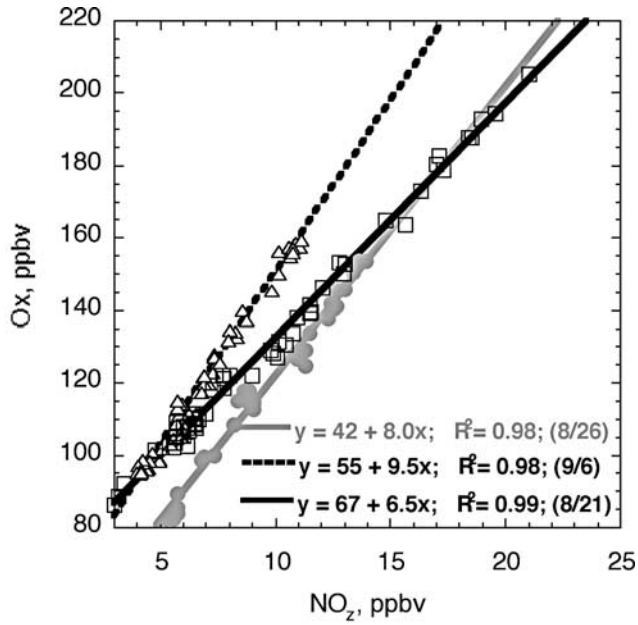

Figure 7. Ox/NO_z regression plots for high O_3 plumes observed on several of the G-1 flights during the TexAQS 2000 study.

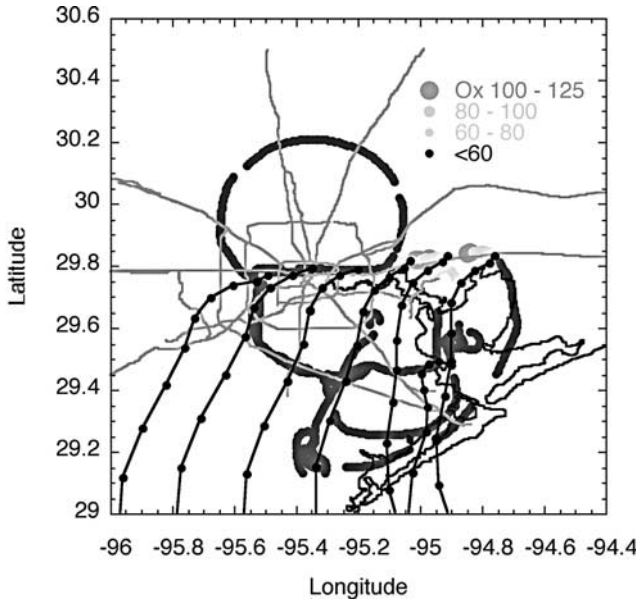

Figure 8. Geographic distribution of oxidant and back trajectories for the morning flight of the G-1 on 26 August 2000 between 09:30 and 12:00 central standard time (CST). Black lines are back trajectories from the indicated locations; black dots on trajectories are spaced at 1 h time intervals. See color version of this figure at back of this issue.

and O_3 distributions for the afternoon flight of the G-1 on 26 August (Figure 2c) indicate that this pool of high O_3 and/or O_3 precursors had been transported from the source region surrounding the Ship Channel some 4–6 hours previous. The G-1 flew over the source region during the morning flight (09:30–12:00 central standard time (CST)) so processes occurring during the morning flight in the source region should be reasonably representative of those that contributed to the pool of ozone observed during the afternoon.

[27] The geographic distribution of Ox for the morning flight of the G-1 is shown in Figure 8. With the exception of the portion of the flight to the north and east of the Ship Channel, Ox concentrations were quite low both in the regional atmosphere surrounding Houston, as well as over downtown Houston. In particular note that Ox was at modest concentrations along the flight track to the northeast of downtown Houston where a high concentration ozone plume was encountered by the G-1 during the afternoon (Figure 2c).

[28] Back trajectories at various times and locations during the morning flight are superimposed on the flight track in Figure 8. These trajectories indicate the region of high ozone concentration observed to the east of Houston can be traced back to emission sources surrounding the Ship Channel. Conversely back trajectories calculated from locations over downtown Houston where low concentrations of ozone were observed were not associated with such sources.

[29] Trace gas concentrations measured during an east-west transect of the metropolitan Houston and the region north of the Ship Channel during late morning (10:15–10:20 CST) are shown in Figure 9. Oxidant concentrations are a modest 40 ppbv over the city but increase dramatically to >100 ppbv over the industrial area surrounding the Ship Channel east of longitude −95.3° (Figure 9, top). The range of NO_x concentrations observed over the Ship Channel is nearly the same as over Houston (Figure 9, bottom) but represents a smaller fraction of the concurrently measured NO_y consistent with consumption of NO_x during ozone formation. Hydrocarbon reactivity over the Ship Channel was considerably higher than over the city. The one urban sample taken on the edge of the industrial area (labeled AM-8 in Figure 9, top) exhibited a hydrocarbon OH reactivity of about 5 s^{-1}. Hydrocarbon reactivities for the Ship Channel samples ranged between circa 10 and 50 s^{-1}, the reactivity of the latter sample was among the highest measured by the G-1 during the entire TexAQS 2000 program. Speciation of the hydrocarbon samples will be discussed below. Formaldehyde concentrations were much higher over the Ship Channel than over the urban area reaching a peak value of nearly 14 ppbv coincident with the

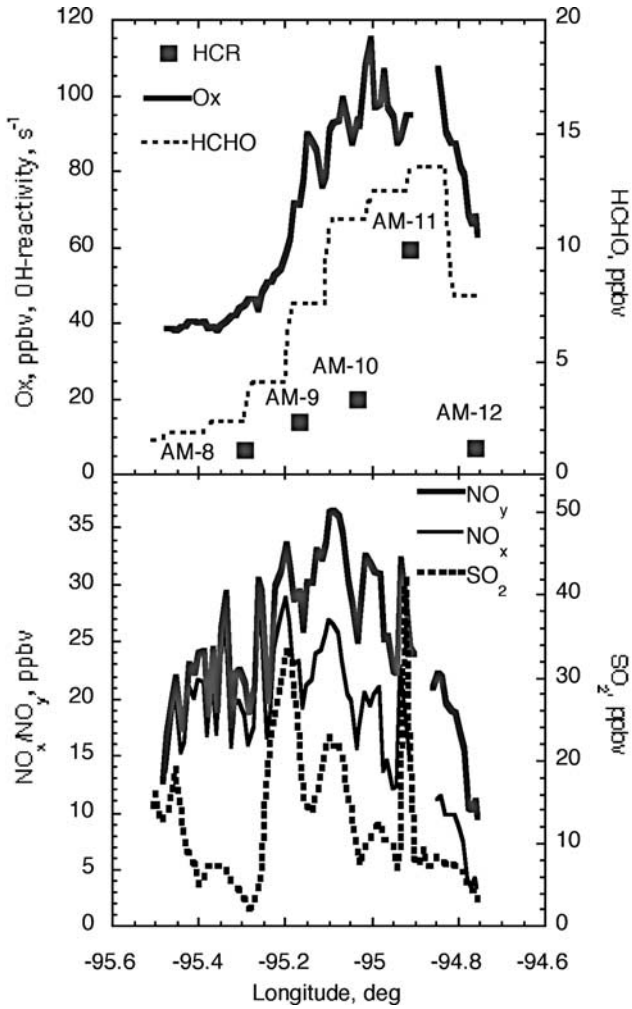

Figure 9. Trace gas concentrations and hydrocarbon reactivities during a G-1 over flight of downtown Houston and the industrial region surrounding the Ship Channel on 26 August 2000, 10:15–10:25 CST. Gaps in the data are due to instrument zeroes.

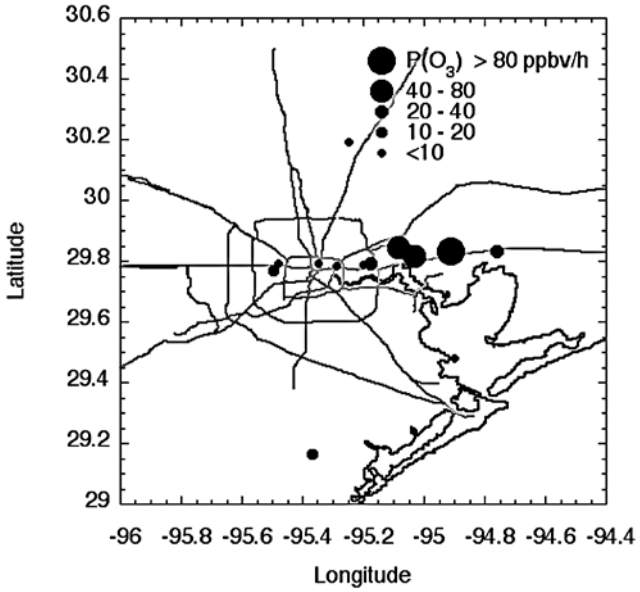

Figure 10. Geographic distribution of values of $P(O_3)$ computed for hydrocarbon canister samples collected during the morning flight of the G-1 on 26 August 2000.

highest reactivity hydrocarbon sample. Formaldehyde concentrations were well correlated with the oxidant concentrations consistent with the results of other analyses of TexAQS 2000 data [*Daum et al.*, 2003; *Ryerson et al.*, 2003; *Wert et al.*, 2003].

[30] Here characteristics of ozone formation in the Ship Channel are examined using a box model constrained by observations as discussed in section 2.3. Although these calculations are sparse, there is an indication that formation rates are much higher over and downwind of the industrial region to the east of Houston than over Houston itself or in the surrounding area (Figure 10). Instantaneous ozone formation rates calculated for some of the samples collected during the afternoon G-1 flight over the Ship Channel were also high. Figure 11 shows the location of hydrocarbon samples during both the morning and afternoon flights for which $P(O_3)$ is >20 ppbv/h. All of these high $P(O_3)$ samples are located close to and downwind of the high emissions region surrounding the Ship Channel.

[31] Precursor concentrations as well as some of the calculated characteristics for the high $P(O_3)$ samples identified in Figure 11 are given in Table 1. $P(O_3)$ for the various samples ranges between 20 and 140 ppbv/h, the latter an extraordinarily high value for $P(O_3)$. Factors driving $P(O_3)$ differ for the various samples. For all of the samples the primary radical production rate Q, is substantial, and a significant fraction derives from photolysis of HCHO; for the sample exhibiting the highest value of $P(O_3)$, Q is very high and a much greater fraction of the radicals originate from HCHO photolysis than from photolysis of O_3, consistent with the high value of HCHO that is associated with this sample (Figure 9, top). It is also clear that a major factor controlling $P(O_3)$ is the hydrocarbon reactivity. All of the high O_3 samples exhibit reactivities that are much higher than observed in samples collected away from the Ship Channel and outside the high ozone plumes that were sampled during the afternoon flight (hydrocarbon OH-reactivity averaged 3.6 and ranged between 1.5 and 5.4 for these samples). For samples exhibiting values of $P(O_3)$ higher than 40 ppbv/h, the hydrocarbon reactivity ranged between 3.3 and 16.5 times the mean value observed in the nonplume, non-Ship Channel samples.

[32] The values of L_N/Q which is a measure of whether $P(O_3)$ is limited by the availability of NO_x or hydrocarbons (a value <0.5 indicating NO_x limited and >0.5 indicating hydrocarbon limited formation) for these high $P(O_3)$ samples varied between 0.99 and 0.41. Three of the samples (AM-10, AM-2, and AM-9) are in the high NO_x regime with L_N/Q near one. For these samples an approximate formula for $P(O_3)$ is

$$P(O_3) = Y\ Qk_1[HC]/k_2[NO_2] \quad (1)$$

where Q is the primary radical production rate; Y is the average yield of $[HO_2] + [RO_2]$ for each OH + HC; $k_1[HC]$ represents the OH reactivity for the mix of hydrocarbons including CO, and $k_2[NO_2]$ is the OH reactivity of NO_2 [*Daum et al.*, 2000a; *Sillman et al.*, 1990; *Sillman*, 1995]. It is the presence of high hydrocarbon reactivity in these high NO_x samples that yields $P(O_3)$ in the range 20–47 ppbv/h, in spite of the inverse NO_x dependence which is suppressing O_3 production. The highest $P(O_3)$ occurs in sample AM-11 with L_N/Q = 0.49, almost at the transition point between NO_x and hydrocarbon sensitive chemistry. The high NO_x formula (1) is a starting point for understanding the cause of the 140 ppbv/h O_3 production rate in sample AM-11. Increasing Q and hydrocarbon reactivity in the 3 high NO_x samples (by factors of 1.7–2.9 and 2.2–4.2, respectively) to yield the conditions for AM-11 causes O_3 production to become more NO_x limited. Although, as L_N/Q decreases, $P(O_3)$ no longer responds linearly to Q and hydrocarbons, each incremental addition of these precursors

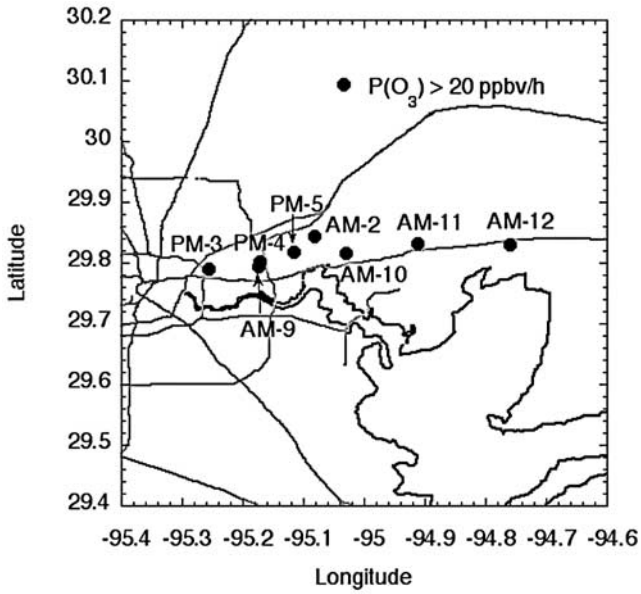

Figure 11. Location of hydrocarbon samples for which $P(O_3)$ > 20 ppbv/h for morning and afternoon flights of the G-1 on 26 August 2000.

Table 1. Characteristics of O_3 Formation for Hydrocarbon Samples Exhibiting $P(O_3) > 20$ ppbv/h on G-1 flights of 26 August 2000

Sample	Time, CST	Q,[a] ppbv/h	NO_x,[b] ppbv	$k_1[HC]$,[c] s^{-1}	$\frac{k_1[HC]}{k_2[NO_2]}$	$P(O_3)$, ppbv/h	L_N/Q[d]	OPEx[e]
AM-11	10:20	10.1 (28/44)	18.0 (0.71)	59.4	16.6	140	0.49	28
AM-10	10:18	5.9 (45/39)	20.4 (0.72)	19.9	5.1	47	0.94	8.5
AM-2	09:05	3.5 (21/22)	20.7 (0.86)	26.7	7.3	45	0.96	13.1
PM-4	13:45	6.8 (64/25)	9.2 (0.47)	12.0	6.7	42	0.62	9.8
PM-5	13:47	6.9 (64/27)	9.9 (0.43)	9.3	4.8	35	0.73	7.0
PM-3	13:42	4.2 (60/25)	7.6 (0.53)	7.1	5.2	27	0.81	7.8
AM-12	10:22	3.9 (55/39)	3.6 (0.37)	7.0	10.2	22	0.41	13.6
AM-9	10:16	3.6 (46/38)	24.9 (0.86)	14.1	3.3	20	0.99	5.7

[a]Primary radical production rate. Values in parentheses show percentage of primary radicals originating from photolysis of O_3 and HCHO, respectively.
[b]Values in parentheses show $\left(\frac{NO_2}{NO_x}\right)$.
[c]Hydrocarbon reactivity toward OH; includes CO and HCHO.
[d]Fraction of radicals removed by reaction with NO_x.
[e]Instantaneous efficiency of O_3 formation calculated as $P(O_3)/P(NO_z)$.

increases $P(O_3)$. The resulting 140 ppbv/h $P(O_3)$ is about 1/2 of the increase that would occur if the response remained linear.

[33] For all of the high $P(O_3)$ samples OPEx, the instantaneous efficiency of ozone formation with respect to NO_x was higher than the range (3–5 ppbv/ppbv) normally observed in a urban plume. Many of the samples had values for OPEx that were 2 to 3 times as high as normally observed in an urban plume; the sample exhibiting the highest value of $P(O_3)$ had an OPEx of 28 (Table 1), so not only was O_3 being produced very rapidly at this location, NO_x was being used very efficiently.

[34] The variation in NO_x or hydrocarbon limited chemistry for the different samples implies that different sources imbedded within the Ship Channel have different emissions characteristics (different NO_x/HC emissions ratios and amounts) that lead to O_3 being formed under different conditions. Understanding such characteristics of individual sources may be important for developing effective control strategies.

[35] Contributions of classes of hydrocarbons to the hydrocarbon OH reactivity associated with the samples listed in Table 1 are shown in Figure 12, ordered by reactivity. For the three samples exhibiting the highest reactivity C2–C4 alkenes contribute most as a class to the hydrocarbon reactivity, and with the exception of the sample exhibiting the lowest reactivity at least one third of the measured reactivity for all of the samples. However, it is important to note that other classes of compounds notably alkanes and HCHO provide significant contributions to hydrocarbon reactivity for some of the samples as well.

3.4.2. 21 August: Ship Channel Plume Advected Over Urban Houston

[36] Data collected during the flights made on 21 August provide another view of the processes associated with formation of high ozone plumes. On 21 August, however, the plume was transported from the Ship Channel over the center of Houston as shown in Figure 2b where it received a fresh injection of NO_x and hydrocarbons, was actively producing O_3, and had the potential for producing significant additional ozone as it was advected to the west. This contrasts with 26 August when the plume was transported from the Ship Channel to a more sparsely populated area where emissions were much lower.

[37] This formation and transport of O_3 was well captured by the surface network as indicated in Figure 13, showing the hourly averaged surface ozone concentration measured in the network in downtown Houston and the surrounding area, as well as, the forward 1 h transport computed from the measured surface winds. Early in the day all of the network sites reported low hourly O_3 concentrations. In Figure 13a, which is for the 11:00–12:00 CST time period, ozone concentrations are all below 80 ppbv except for two sites around the Ship Channel, and two sites well to the east. In the succeeding plots more and more of the sites exhibit elevated O_3 concentrations and it is apparent that the region of high ozone concentration is moving from east to west with peak ozone concentrations of over 150 ppbv hourly average observed within the metropolitan area between 13:00 and 15:00 CST. This westward movement is consistent both with the back trajectory shown in Figure 2b, and with the surface winds. Toward late afternoon, the region of high O_3 concentration had moved almost entirely out of Houston and O_3 concentrations gradually returned to more moderate levels starting from the east and gradually extending to the west.

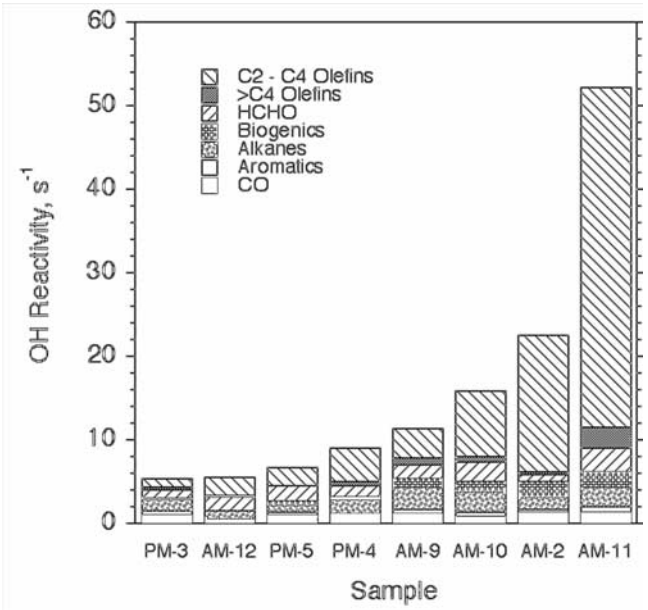

Figure 12. Apportionment of reactivity for hydrocarbon samples exhibiting $P(O_3) > 20$ ppbv/h collected by the G-1 on 26 August 2000.

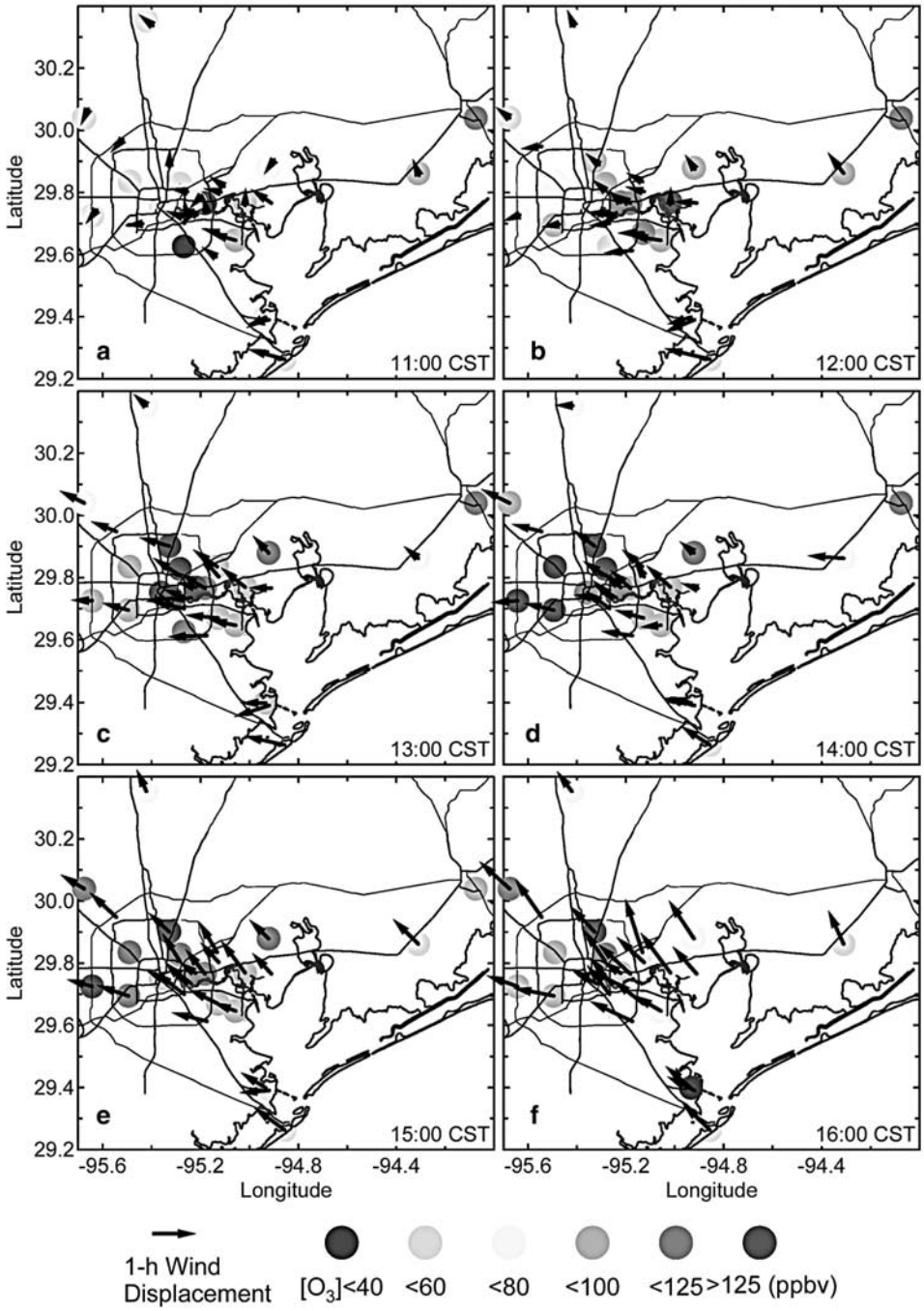

Figure 13. Hourly averaged O_3 concentrations measured at surface sites in the greater Houston metropolitan area on 21 August 2000. Arrows represent the direction and magnitude of the subsequent 1-h transport from the sites as computed from the measured surface winds. See color version of this figure at back of this issue.

[38] Three aircraft flights were made on 21 August; two by the Twin Otter and one by the G-1. The first flight by the Twin Otter started at 0730 CST and ended at 1000 CST; the second between 1300 and 1530 CST. The G-1 flew a single flight between 1330 and 1600 CST.

[39] Boundary layer O_3 concentrations (not shown) observed during the first Twin Otter flight were quite low ranging between 20 and 50 ppbv, the lower values, a consequence of titration by NO emissions. The atmosphere was stratified with a strong inversion observed at circa 750 m. Above this altitude the relative humidity decreased rapidly and ozone concentrations rose sharply to nearly 80 ppbv. NO_x concentrations aloft were quite low indicating that this was an aged air mass with little potential for formation of additional ozone. The geographic distribution of the hydrocarbon reactivity as derived from canister samples collected on the flight are shown in Figure 14a. Although sparse, these samples indicate the presence of

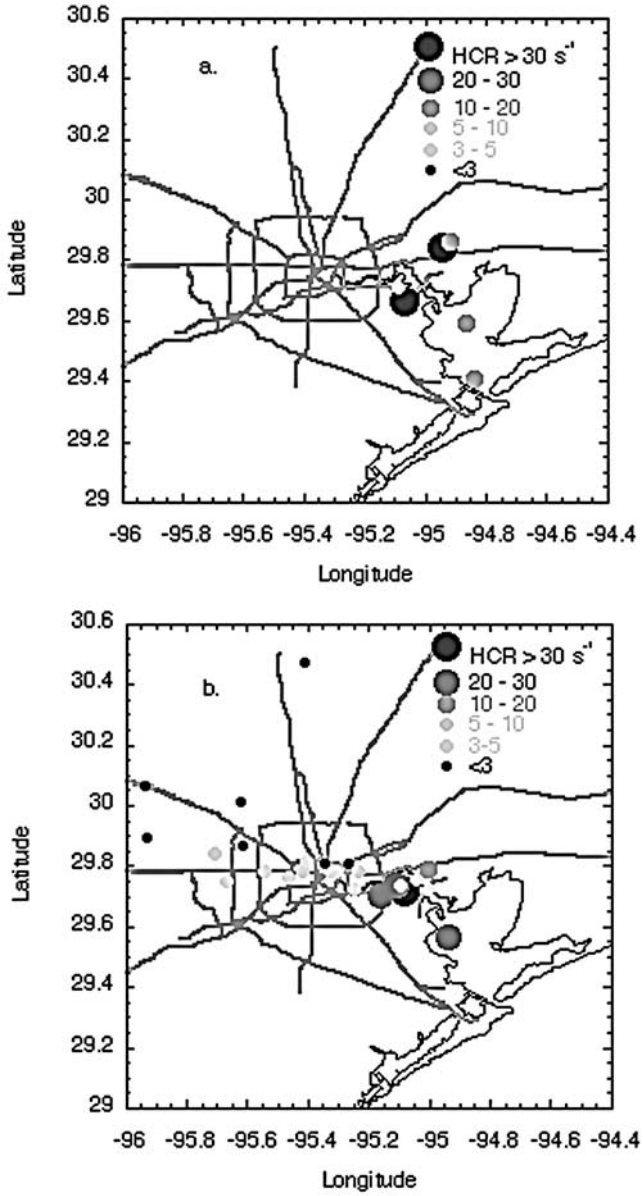

Figure 14. Hydrocarbon reactivities measured by aircraft on 21 August 2000. (a) Measurements from the early morning flight of the Twin Otter. (b) Measurements from the afternoon flights of the G-1 and the Twin Otter. See color version of this figure at back of this issue.

high hydrocarbon reactivities over Galveston Bay and around the Houston Ship Channel.

[40] The afternoon flights of the Twin Otter and the G-1 were nearly concurrent, but as indicated by the flight tracks shown in Figures 15 and 16, the Twin Otter focused on the region around the Ship Channel, and Galveston Bay whereas the G-1 flight was more far ranging. The geographic distribution of the aircraft ozone concentrations was very similar to the pattern exhibited by the ozone concentrations measured at the surface sites (Figures 13c and 13d) with high concentrations of ozone from the Ship Channel west over downtown Houston and much lower concentrations elsewhere. Figure 14b shows the geographic distribution of the hydrocarbon reactivities derived from the canisters collected on the afternoon flights of both the G-1 and the Twin Otter. These hydrocarbon reactivities exhibit a gradient that runs from east to west, with somewhat higher concentrations in the east and lower concentrations to the west consistent with the east/west flow and with industries surrounding the Ship Channel serving as a source of both

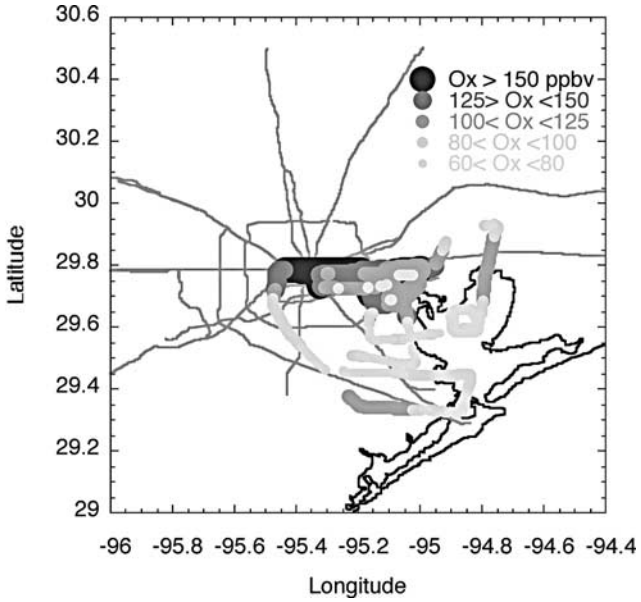

Figure 15. Geographic distribution of Ox measured during the afternoon flight of the Twin Otter on 21 August 2000. See color version of this figure at back of this issue.

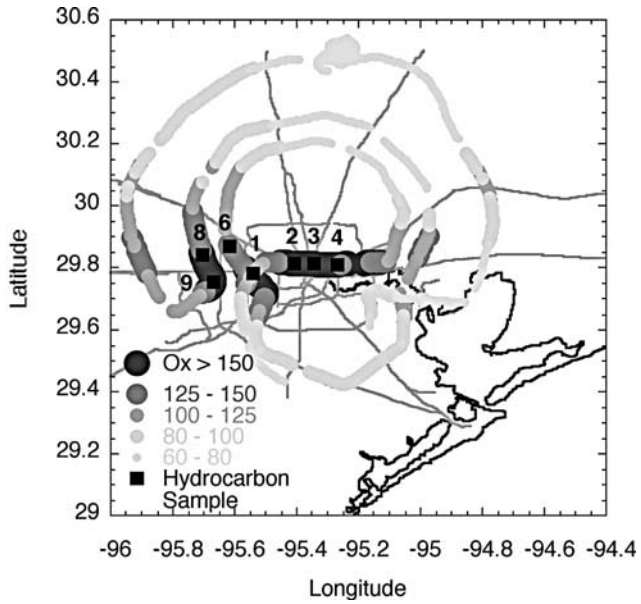

Figure 16. Geographic distribution of Ox measured during the afternoon flight of the G-1 on 21 August 2000. Black squares indicate location and identity of hydrocarbon canister samples. See color version of this figure at back of this issue.

Table 2. Instantaneous Chemistry Derived From Constrained Box Model Calculations in the High O_3 Plume Observed Over Downtown Houston on 21 August 2000

Sample	Time, CST	Q,[a] ppbv/h	NO_x,[b] ppbv	O_3, ppbv	$k_1[HC]$,[c] s^{-1}	$\frac{k_1[HC]}{k_2[NO_2]}$	$P(O_3)$, ppbv/h	L_N/Q[d]	OPEx[e]
1	13:44	5.0 (68/19)	13.1 (0.53)	100	8.8	3.6	26	0.93	5.5
2	13:47	8.3 (70/19)	8.4 (0.34)	177	9.4	5.6	36	0.54	6.7
3	13:48	6.9 (76/18)	6.1 (0.32)	155	6.2	5.1	21	0.53	5.7
4	13:49	7.0 (75/16)	4.1 (0.26)	150	6.5	7.9	17	0.33	7.5
6	14:11	5.1 (71/16)	7.0 (0.41)	122	5.1	3.8	20	0.73	5.2
8	14:55	5.9 (62/16)	8.5 (0.41)	147	7.5	4.5	24	0.65	6.3
9	14:57	5.3 (73/18)	7.0 (0.29)	167	6.9	5.0	18	0.57	5.8

[a]Primary radical production rate. Values in parentheses are percentage of primary radicals originating from photolysis of O_3 and HCHO, respectively.
[b]Values in parentheses show $\left(\frac{|NO_2|}{|NO_x|}\right)$.
[c]Hydrocarbon reactivity toward OH; includes CO and HCHO.
[d]Fraction of radicals removed by reaction with NO_x.
[e]Instantaneous efficiency of O_3 formation calculated as $P(O_3)/P(NO_z)$.

NO_x and hydrocarbons. Presumably, there is also a gradient in $P(O_3)$, but there is insufficient data associated with the hydrocarbon canisters collected by the Twin Otter to adequately constrain the calculations.

[41] Results of box model calculations for hydrocarbon samples collected in the high O_3 portion of the plume observed on 21 August by the G-1 are given in Table 2. Geographic location and identity of these samples is shown in Figure 16. As indicated in Table 2, values of $P(O_3)$ are high, ranging between 17 and 36 ppbv/h despite the fact that significant O_3 had already formed and that NO_x concentrations had already been significantly depleted. Values of OPEx were higher than usually observed in a late afternoon urban plume but lower than we typically observed in the Ship Channel Plume on other days (e.g., section 3) [*Daum et al.*, 2003]. Hydrocarbon reactivities were higher than we observed directly over the urban area on other days [e.g., *Daum et al.*, 2003], but not as high on average, as we observed directly over the Ship Channel [*Kleinman et al.*, 2002a; *Daum et al.*, 2003]. Values of L_N/Q ranged between 0.33 and 0.93 and averaged 0.61; on other days (e.g., 29 August [*Daum et al.*, 2003]) L_N/Q averaged >0.9 for samples collected directly over the urban area. Thus it appears that $P(O_3)$ over the urban area on the afternoon of 21 August was much less hydrocarbon limited than it was on other days. It is also worth noting that the high O_3 plume observed on 21 August during midafternoon had sufficient NO_x and hydrocarbons (Table 2) to generate significant additional O_3 before photochemistry shut down for the day.

[42] The O_3 exceedance that occurred on 21 August, in many senses represents a worst case scenario for O_3 formation in the Houston area. Ozone and precursors accumulated over the Ship Channel during the morning and early afternoon, and were then transported directly over the urban area where they received a fresh injection of NO_x and hydrocarbons from vehicular sources which sustained the O_3 formation process and allowed for the formation of substantial additional O_3.

4. Hydrocarbon and NO_x Limitations to Ozone Formation

[43] Whether maximum O_3 concentrations are determined by NO_x or hydrocarbon emissions is important from the perspective of developing effective control strategies. In most large urban areas in the U.S. the maximum amount of O_3 formed is limited by the availability of hydrocarbons and control strategies have been focused on reduction of hydrocarbon emissions. Because of the intense hydrocarbon sources in the Houston area the question arises as to whether this strategy also applies to Houston. The usual mechanism for determining optimal control strategies is through use of photochemical/transport models driven by emissions and meteorological fields specific for a given area. Since reported hydrocarbon emissions for industrial facilities surrounding Houston are thought to be low by a factor of 10 or more [*Ryerson et al.*, 2003; *Wert et al.*, 2003], such modeling exercises cannot yet give useful insight as to how best to control Houston's ozone problem. Here we examine the instantaneous chemistry, and the distribution of photochemical product species to develop insight as to what the most effective control strategy might be.

[44] The instantaneous chemistry as inferred from our constrained box model calculations is examined first. Under the assumption that regions of high $P(O_3)$ will contribute most to the regions of high O_3 concentrations that were observed, we examine hydrocarbon/NO_x limitations to the instantaneous chemistry for all of the high $P(O_3)$ samples (defined as any sample for which $P(O_3) > 15$ ppbv/h) contained within our data set. About 25% of the samples that were collected by the G-1 fell within this category; most of these high $P(O_3)$ samples were either in the vicinity of the Ship Channel, or were no more than a few hours downwind of the Ship Channel as determined by back trajectory analysis. One output of the calculations is the quantity L_N/Q which as mentioned above, is an indicator of NO_x ($L_N/Q < 0.5$) or hydrocarbon ($L_N/Q > 0.5$) sensitivity of the instantaneous chemistry. About 22% of the high $P(O_3)$ samples exhibited values of $L_N/Q < 0.5$; and about 40% of the samples exhibited values <0.6 indicating that there is tendency toward NO_x limited O_3 production in Houston that is not observed in other urban areas that we have studied. All of the high $P(O_3)$ samples having L_N/Q values <0.5 were geographically located in the Ship Channel industrial region or close by downwind. Characteristics of these samples include a $P(O_3)$ that ranges between 15 and 140 ppbv/h, median 39 ppbv/h; NO_x concentrations that range between 2.6 and 18 ppbv, median 6.6 ppbv, and; L_N/Q values that range between 0.28 and 0.50, median 0.42. The observation of substantial rates of O_3 production under NO_x limited conditions in a major ozone precursor source region suggests that there are individual sources, or combi-

Table 3. Values of Indicator Ratios Computed for High O_3 Plumes Observed by the G-1 During the TexAQS 2000 Study

Day	Total Peroxide/NO_z[a]	$\Delta O_3/\Delta NO_z$[b]
19 August	1.0	10–12
21 August	—	7
26 August	0.6–0.9	9.5–12
29 August	0.5–1.3	10–13
31 August	0.8–1.0	8.5
6 September	—	11

[a]Median value of total peroxide/NO_z for simulations reported by *Sillman and He* [2002] is 0.2 for HC and 0.8 for NO_x-sensitive O_3 formation.

[b]Median value of $\Delta O_3/\Delta NO_z$ for simulations reported by *Sillman and He* [2002] is 4.5 for HC and 8.5 for NO_x-sensitive O_3 formation.

nation of sources that produce O_3 under NO_x limited conditions, but does not answer the question of whether the magnitude of peak O_3 concentrations as observed during the flights discussed here are limited by the availability of NO_x or hydrocarbons.

[45] Another way to examine NO_x or hydrocarbon limitations to O_3 formation is through use of indicator ratios [*Sillman and He*, 2002; *Sillman et al.*, 1995; *Sillman*, 1990] which are ratios of concentrations of various photochemical product species. The indicator ratios t-peroxide/NO_z, where t-peroxide is the sum of H_2O_2 and organic peroxides, and $\Delta O_3/\Delta NO_z$ will be used here. The indicator ratio t-peroxide/NO_z is thought to be one of the most robust and direct indicators of NO_x/hydrocarbon sensitivity; $\Delta O_3/\Delta NO_z$ is somewhat less direct and robust, but is included here for comparative purposes and because we do not have measurements of t-peroxide for all of the high O_3 plumes that are discussed here. To give a sense of whether values of these ratios indicate NO_x or VOC sensitivity, we note that the median value of the 50th percentile of simulations for VOC sensitive locations of the indicator ratio t-peroxide/NO_z is 0.21, $\sigma = 0.035$ and for the 50th percentile of NO_x sensitive locations is 0.8, $\sigma = 0.22$; equivalent values for the indicator ratio $\Delta O_3/\Delta NO_z$ are 4.5, $\sigma = 1.0$ and 8.5, $\sigma = 1.8$ [*Sillman and He*, 2002] (Table 2).

[46] Values of t-peroxide/NO_z and $\Delta O_3/\Delta NO_z$ were calculated for all of the high ozone plumes sampled during the program for which t-peroxide was measured; results are given in Table 3. Values of t-peroxide/NO_z shown in Table 3 suggest that O_3 formation in the high ozone plumes in which this ratio was measured are much closer to being limited by the availability of NO_x, than hydrocarbons. A similar view is obtained from values of $\Delta O_3/\Delta NO_z$ which, with the exception of 21 August, exhibit values that are equal to, or higher than 8.5. The lower values on 21 August with respect to other days is consistent with the admixture of fresh NO_x from vehicle emissions as discussed above, which would cause O_3 formation to be somewhat less NO_x limited than might otherwise be the case.

[47] Although both the instantaneous chemistry and the indicator ratios indicate a tendency of O_3 formation to be NO_x limited in some of the high ozone plumes found in and around Houston, these results are by no means definitive. Development of effective control strategies for the Houston area will require use of sophisticated chemical transport models with accurate emissions inventories. The latter will require substantial improvement of inventories that are currently used to develop Houston ozone control strategies [*Ryerson et al.*, 2003].

5. Summary

[48] The G-1 made flights on 13 days during the month long TexAQS 2000 program. On six of those days the aircraft sampled plumes exhibiting O_3 concentrations in excess of 150 ppbv. These plumes were encountered at a number of different locations in and around the greater Houston area. The composition of these plumes differed significantly from those typically observed in urban areas, exhibiting unusually high concentrations of hydrocarbon oxidation products such as HCHO (up to 30 ppbv), and photochemical product species such as peroxides (up to 16 ppbv). The former is a principal product of the degradation of low molecular weight alkenes, and the latter is an important indicator of the occurrence of NO_x limited O_3 formation. Estimates of the integrated formation efficiency of O_3 with respect to NO_x from Ox/NO_z regressions indicated that O_3 had been formed in these high concentration plumes with efficiencies ranging between 6.4 and 11 ppbv O_3 per ppbv of NO_x consumed. These efficiencies are much higher than the range of values (3–5) we have observed in mature urban plumes in other studies.

[49] Without exception, back trajectories from the locations where these high O_3 plumes were observed passed over, or in close proximity to, sources of NO_x and hydrocarbons surrounding the Houston Ship Channel suggesting that these sources made a significant contribution to the O_3 that had been formed. The characteristics of the high O_3 plumes were linked to processes occurring over the Ship Channel on several high O_3 days when the G-1 sampled the Ship Channel area during the morning hours. For the two days that were examined in detail, box model calculations indicated that there were regions in the Ship Channel where O_3 formation was very rapid (up to 140 ppbv/h) and very efficient (OPEx up to 28).

[50] Both the instantaneous chemistry, and the distribution of photochemical product species were examined with regard to NO_x or hydrocarbon limitations to O_3 formation. A significant fraction ~20% of the high $P(O_3)$ samples ($P(O_3) > 15$ ppbv/hr) exhibited NO_x limited O_3 formation rates. All of these samples were located in and around the Houston Ship Channel. This suggests that there are sources or combinations of sources that can lead to NO_x limited chemistry, but does not address the question of whether peak O_3 in the high O_3 plumes is limited by the availability of NO_x or hydrocarbons. Examination of the distribution of photochemical product distributions in the high O_3 plumes indicates a tendency toward NO_x limited behavior in some of the high O_3 plumes, but chemical/transport model simulations with realistic emissions inventories are needed to resolve the NO_x/hydrocarbon limited question. Analysis of the data presented here suggest that often, the plumes of high O_3 observed by the G-1 during the TexAQS 2000 are formed according to the following scenario. During the early morning, winds are low, emissions of NO_x and hydrocarbons from the industrial facilities around northern Galveston Bay and the Houston Ship Channel and from mobile sources in the area accumulate. The mix of O_3 precursors is such that as soon as the actinic flux is sufficiently high,

ozone is formed at very high rates and efficiencies. This pool of hydrocarbons and NO_x and accumulated O_3 is then moved by the developing sea breeze in the middle to late afternoon to another location within in the Houston area where it is observed as a region of high O_3 concentration. These findings are consistent with those reported elsewhere in a detailed case study analysis of the data collected on 29 August [*Daum et al.*, 2003].

[51] **Acknowledgments.** This study was supported by funding from the U.S. Department of Energy through the Atmospheric Chemistry Program, U.S. Environmental Protection Agency through the Southern Oxidants Study, and by the Texas Commission on Environmental Quality. This research was performed under sponsorship of the U.S. Department of Energy under sponsorship of the U.S. DOE under contracts DE-AC02-98CH10886 and DOE FG02-98ER.

References

Daum, P. H., L. Kleinman, D. G. Imre, L. J. Nunnermacker, Y.-N. Lee, S. R. Springston, and L. Newman (2000a), Analysis of the processing of Nashville urban emissions on July 3 and July 18, 1995, *J. Geophys. Res.*, *105*, 9155–9164.

Daum, P. H., D. G. Imre, L. I. Kleinman, Y.-N. Lee, L. J. Nunnermacker, and S. R. Springston (2000b), Comparison of ozone production rates and efficiencies in Nashville and Phoenix, *Eos Trans. AGU*, *81*(48), Fall Meet. Suppl., Abstract A71E-03.

Daum, P. H., L. I. Kleinman, S. R. Springston, L. J. Nunnermacker, Y.-N. Lee, J. Weinstein-Lloyd, J. Zheng, and C. Berkowitz (2003), A comparative study of O_3 formation in the Houston urban and industrial plumes during the TEXAQS 2000 Study, *J. Geophys. Res.*, *108*(D23), 4715, doi:10.1029/2003JD003552.

Harley, R. A., et al. (2001), Analysis of motor vehicle emissions, *J. Geophys. Res.*, *106*, 3559–3567.

Jobson, B. T., G. J. Frost, S. McKeen, T. B. Ryerson, M. P. Buhr, D. D. Parrish, M. Trainer, and F. C. Fehsenfeld (1998), Hydrogen peroxide dry deposition lifetime determined from observed loss rates in a power plant plume, *J. Geophys. Res.*, *103*, 22,617–22,628.

Karl, T., T. Jobson, W. C. Kuster, E. Williams, J. Stutz, R. Shetter, S. R. Hall, P. Goldan, F. Fehsenfeld, and W. Lindinger (2003), Use of proton-transfer-reaction mass spectrometry to characterize volatile organic compound sources at the La Porte super site during the Texas Air Quality Study 2000, *J. Geophys. Res.*, *108*(D16), 4508, doi:10.1029/2002JD003333.

Kleinman, L. I., P. H. Daum, J. H. Lee, Y.-N. Lee, L. J. Nunnermacker, S. R. Springston, L. Newman, J. Weinstein-Lloyd, and S. Sillman (1997), Dependence of ozone production on NO and hydrocarbons in the troposphere, *Geophys. Res. Lett.*, *24*, 2299–2302.

Kleinman, L. I., P. H. Daum, D. G. Imre, J. H. Lee, Y.-N. Lee, L. J. Nunnermacker, S. R. Springston, J. Weinstein-Lloyd, and L. Newman (2000), Ozone production in the New York City urban plume, *J. Geophys. Res.*, *105*(11), 14,495–14,511.

Kleinman, L. I., P. H. Daum, Y.-N. Lee, L. J. Nunnermacker, S. R. Springston, J. Weinstein-Lloyd, and J. Rudolph (2001), Sensitivity of ozone production rate to ozone precursors, *Geophys. Res. Lett.*, *28*, 2903–2906.

Kleinman, L. I., P. H. Daum, D. Imre, Y.-N. Lee, L. J. Nunnermacker, S. R. Springston, J. Weinstein-Lloyd, and J. Rudolph (2002a), Ozone production rate and hydrocarbon reactivity in 5 urban areas: A cause of high ozone concentration in Houston, *Geophys. Res. Lett.*, *29*(10), 1467, doi:10.1029/2001GL014569.

Kleinman, L. I., P. H. Daum, Y.-N. Lee, L. J. Nunnermacker, S. R. Springston, J. Weinstein-Lloyd, and J. Rudolph (2002b), Ozone production efficiency in an urban area, *J. Geophys. Res.*, *107*(D23), 4733, doi:10.1029/2002JD002529.

Lee, Y.-N., et al. (1998), Atmospheric chemistry and distribution of formaldehyde and several multi-oxygenated carbonyl compounds during the 1995 Nashville/middle Tennessee ozone study, *J. Geophys. Res.*, *103*, 22,449–22,462.

Nielson-Gammon, J. (2002), Meteorological modeling of a Houston ozone episode, *Eos Trans. AGU*, *83*(47), Fall Meet. Suppl., Abstract A21F-01.

Nunnermacker, L. J., et al. (1998), Characterization of the Nashville urban plume on July 3 and July 18, 1995, *J. Geophys. Res.*, *103*, 28,129–28,148.

Paulson, S. E., and J. H. Seinfeld (1992), Development and evaluation of a photochemical mechanism for isoprene, *J. Geophys. Res.*, *97*, 20,703–20,715.

Rudolph, J. (1999), Measurements of nonmethane hydrocarbons in the atmosphere, in *Volatile Organic Compounds in the Troposphere, Schr. Forschungzentrum Julich*, *Reihe Umwelt/Environ.*, vol. 16, edited by R. Koppman and D. H. Ehhalt, pp. 11–35, Forschungszentrum Jülich, Jülich, Germany.

Rudolph, J., and A. Khedim (1985), Hydrocarbons in the non-urban atmosphere: Analysis, ambient concentrations and impact on the chemistry of the atmosphere, *Int. J. Environ. Anal. Chem.*, *20*, 265–282.

Ryan, W. F., B. G. Doddridge, R. R. Dickerson, R. M. Morales, K. A. Hallock, P. T. Roberts, D. L. Blumenthal, J. A. Anderson, and K. L. Civerolo (1998), Pollutant transport during a regional O_3 episode in the Mid-Atlantic states, *J. Air Waste Manage. Assoc.*, *48*, 786–797.

Ryerson, T. B., et al. (2003), Effect of petrochemical industrial emissions of reactive alkenes and NO_x on tropospheric ozone formation in Houston, Texas, *J. Geophys. Res.*, *108*(D8), 4249, doi:10.1029/2002JD003070.

Sillman, S. (1995), Use of NO_y, HCHO, H_2O_2 and HNO_3 as indicators for ozone-NO_x-hydrocarbon sensitivity in urban locations, *J. Geophys. Res.*, *100*, 14,175–14,188.

Sillman, S., and D. He (2002), Some theoretical results concerning O_3-NO_x-VOC chemistry and NO_x-VOC indicators, *J. Geophys. Res.*, *107*(D22), 4659, doi:10.1029/2001JD001123.

Sillman, S., J. A. Logan, and S. C. Wofsy (1990), The sensitivity of ozone to nitrogen oxides and hydrocarbons in regional ozone episodes, *J. Geophys. Res.*, *95*, 1837–1851.

Stockwell, W. R., P. Middleton, J. S. Chang, and X. Tang (1990), The second generation regional acid deposition model chemical mechanism for regional air quality modeling, *J. Geophys. Res.*, *95*, 16,343–16,367.

Sueper, D., et al. (2002), Intercomparison of chemical trace species measured on the Electra during TexAQS 2000, *Eos Trans. AGU*, *83*(47), Fall Meet. Suppl., Abstract A12D-0182.

Weinstein-Lloyd, J., J. H. Lee, P. H. Daum, L. I. Kleinman, L. J. Nunnermacker, S. R. Springston, and L. Newman (1998), Measurements of peroxides and related species during the 1995 summer intensive of the Southern Oxidants Study in Nashville, Tennessee, *J. Geophys. Res.*, *103*, 22,361–22,374.

Wert, B. P., et al. (2003), Signatures of terminal alkene oxidation in airborne formaldehyde measurements during TexAQS 2000, *J. Geophys. Res.*, *108*(D3), 4104, doi:10.1029/2002JD002502.

Zhang, J., S. T. Rao, and S. M. Daggupaty (1998), Meteorological processes and ozone exceedances in the northeastern United States during the 12–16 July 1995 episode, *J. Appl. Meteorol.*, *37*, 776–789.

C. M. Berkowitz, Atmospheric Sciences and Global Change Division, Pacific Northwest National Laboratory, P.O. Box 999, Richland, WA 99352, USA.

P. H. Daum, L. I. Kleinman, Y.-N. Lee, L. J. Nunnermacker, and S. R. Springston, Environmental Sciences Department, Atmospheric Sciences Division, Brookhaven National Laboratory, Upton, NY 11973-5000, USA. (phdaum@bnl.gov)

J. Weinstein-Lloyd, Chemistry and Physics Department, State University of New York at Old Westbury, Old Westbury, NY 11568, USA.

J. Zheng, Institute for Terrestrial and Planetary Atmospheres, State University of New York at Stony Brook, Stony Brook, NY 11794, USA.

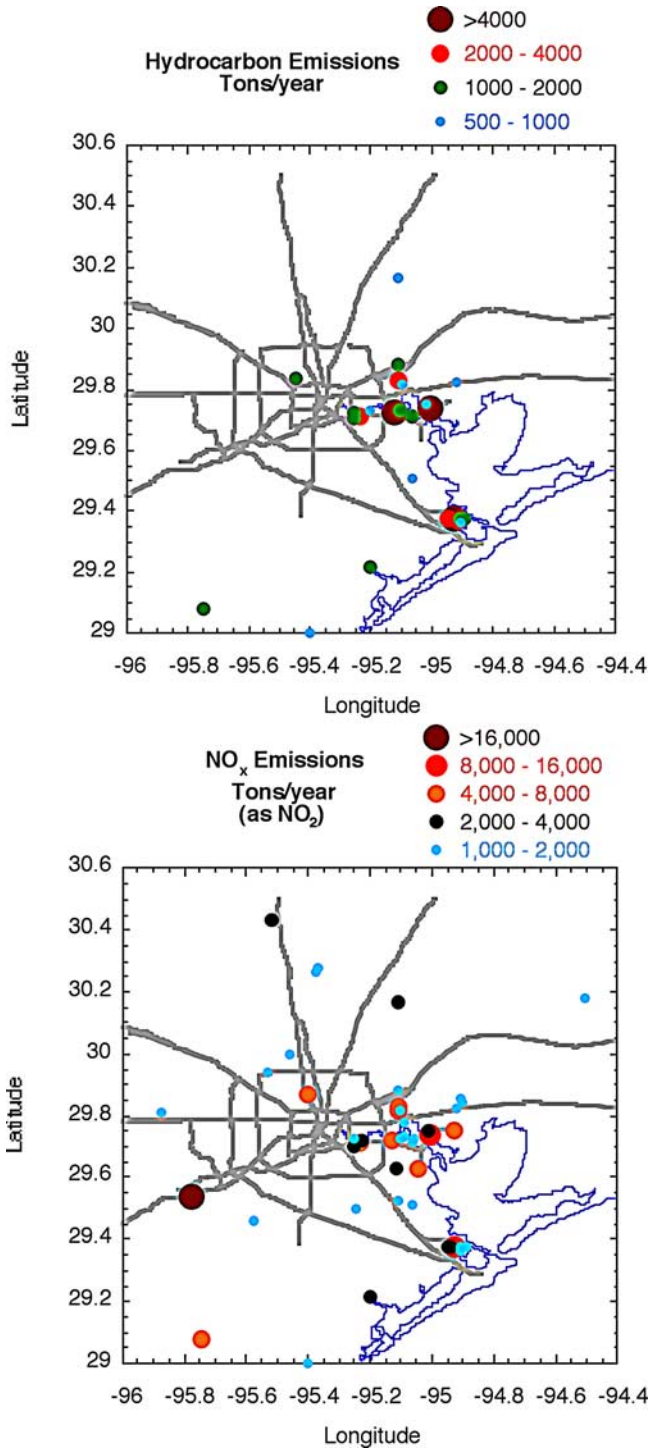

Figure 1. Geographic distribution of hydrocarbon and NO_x point sources in the Houston/Galveston area. Sources of hydrocarbons below 500 tons per year and NO_x below 1000 tons per year are not shown.

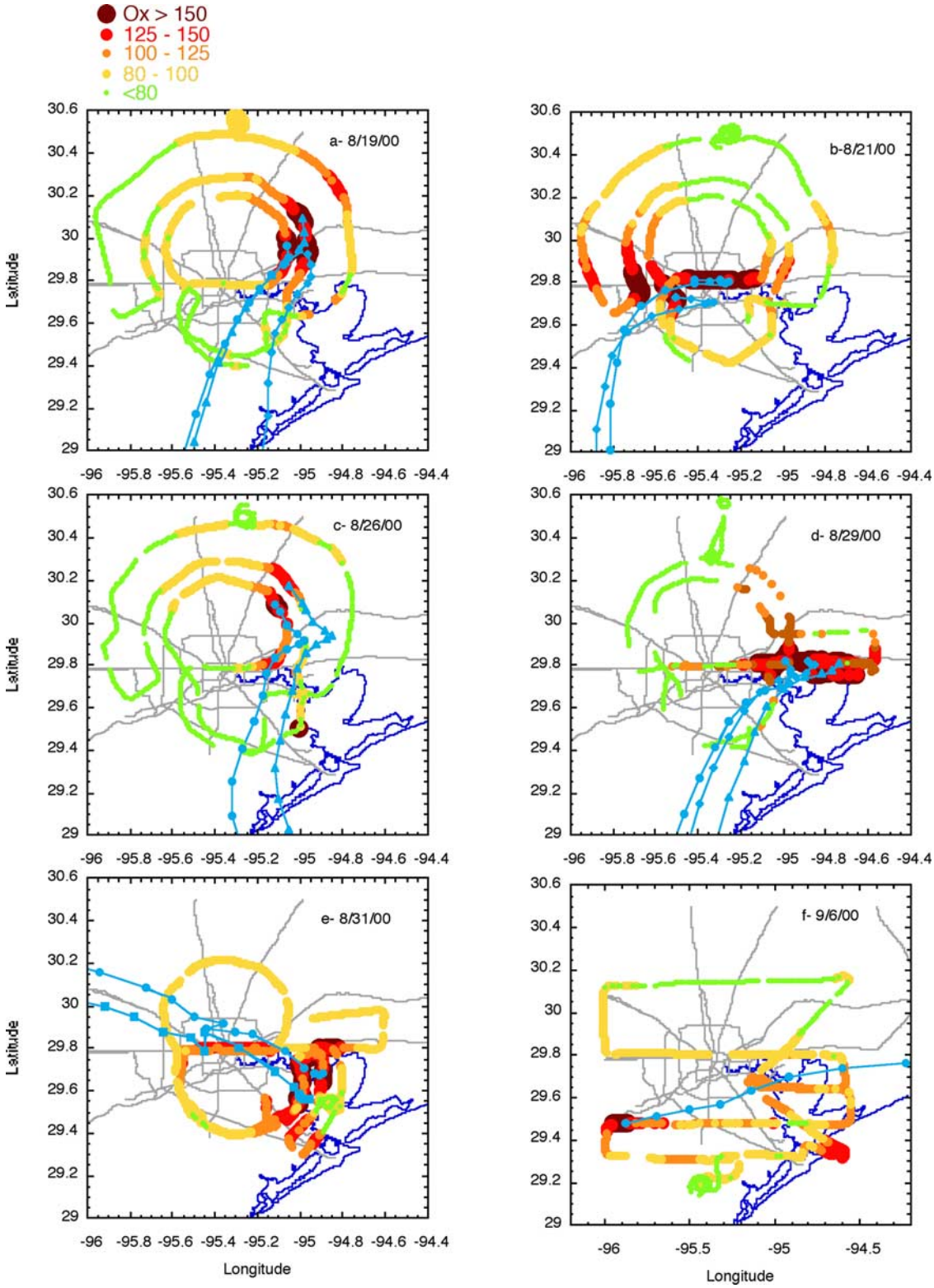

Figure 2. Geographic distribution of Ox for G-1 flights during which O_3 concentrations were >150 ppbv. Blue lines are back trajectories from the indicated locations of high Ox. Symbols on the trajectories are spaced at 1-h intervals. Read 8/19/00 as 19 August 2000.

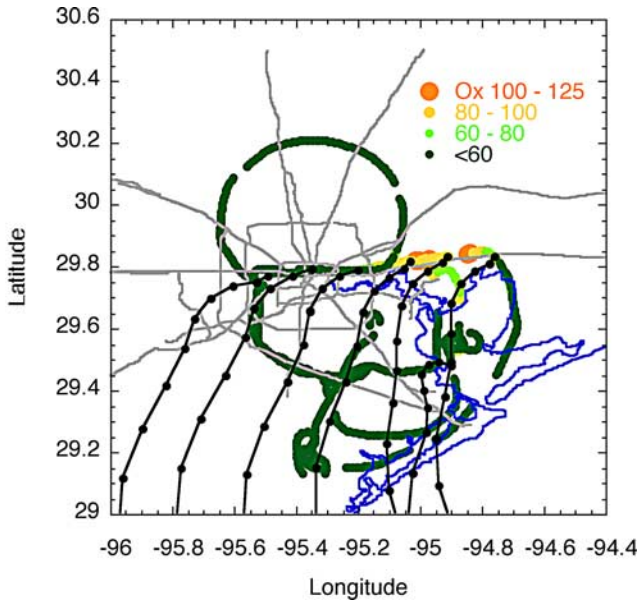

Figure 8. Geographic distribution of oxidant and back trajectories for the morning flight of the G-1 on 26 August 2000 between 09:30 and 12:00 central standard time (CST). Black lines are back trajectories from the indicated locations; black dots on trajectories are spaced at 1 h time intervals.

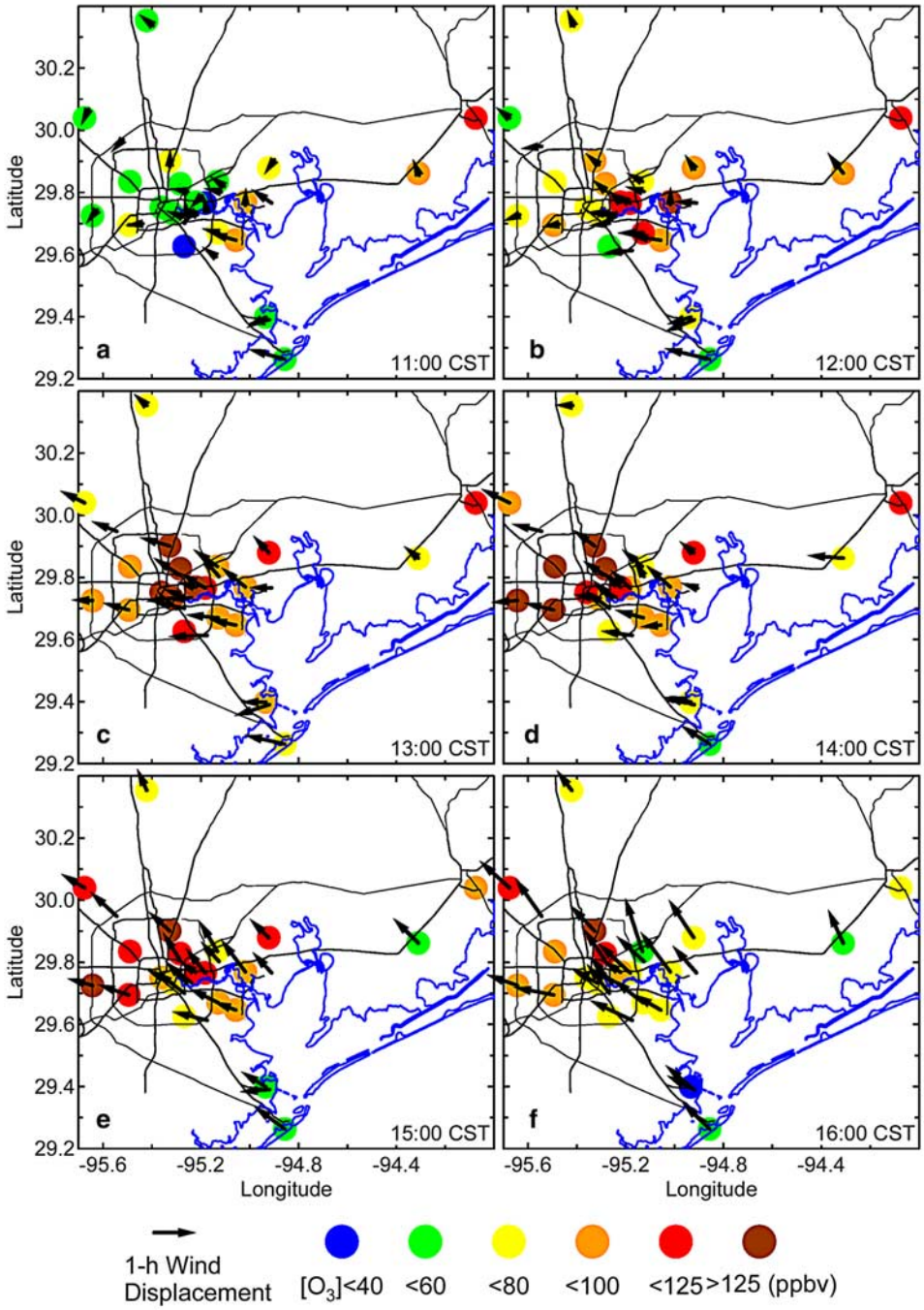

Figure 13. Hourly averaged O_3 concentrations measured at surface sites in the greater Houston metropolitan area on 21 August 2000. Arrows represent the direction and magnitude of the subsequent 1-h transport from the sites as computed from the measured surface winds.

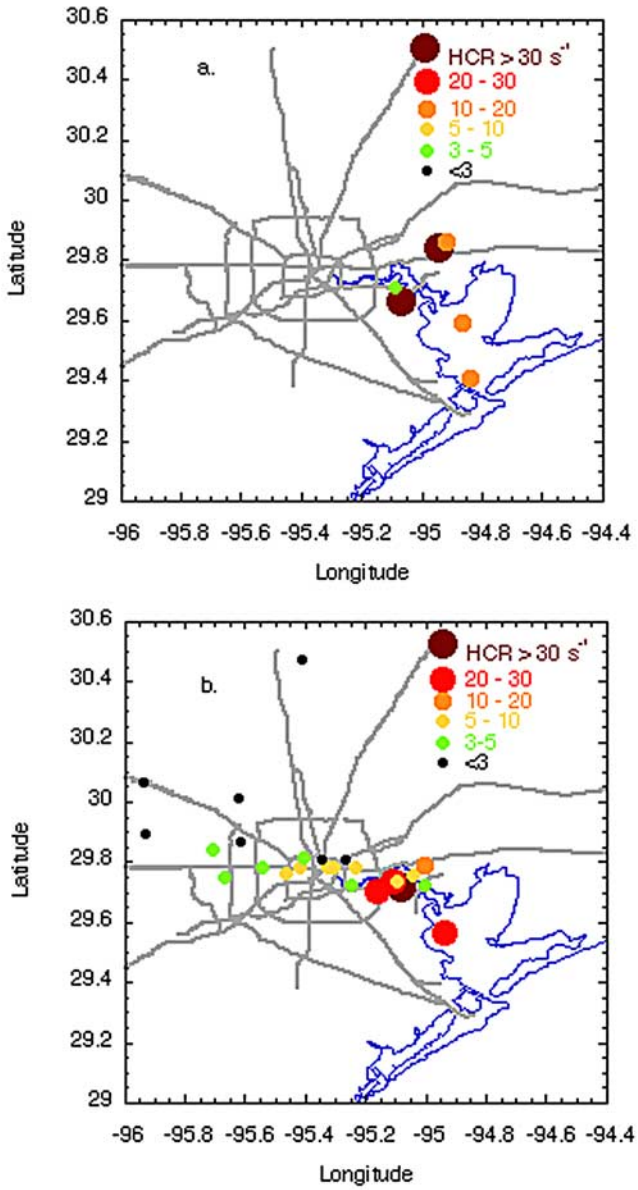

Figure 14. Hydrocarbon reactivities measured by aircraft on 21 August 2000. (a) Measurements from the early morning flight of the Twin Otter. (b) Measurements from the afternoon flights of the G-1 and the Twin Otter.

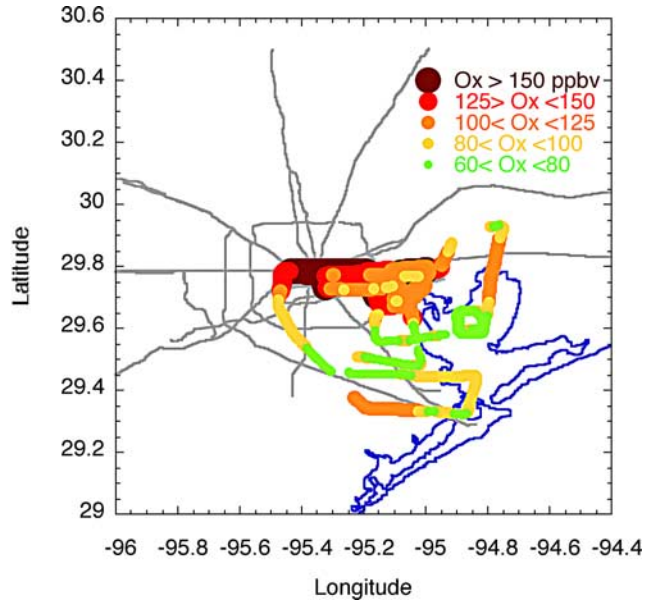

Figure 15. Geographic distribution of Ox measured during the afternoon flight of the Twin Otter on 21 August 2000.

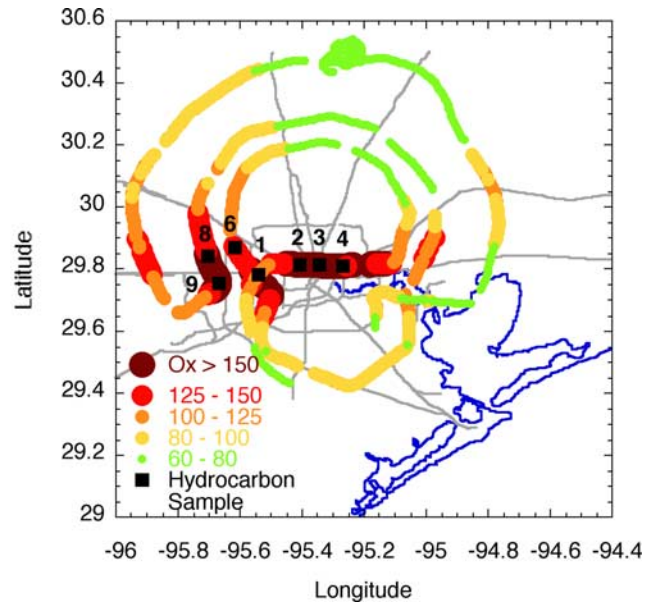

Figure 16. Geographic distribution of Ox measured during the afternoon flight of the G-1 on 21 August 2000. Black squares indicate location and identity of hydrocarbon canister samples.